BMC Genomics

RESEARCH

Open Access

Characterization and expression analysis of the *B3* gene family during seed development in *Akebia trifoliata*

Huijuan Liu[1,2], Jinling Li[2], Cunbin Xu[2], Hongchang Liu[2] and Zhi Zhao[2*]

Abstract

Background *B3* genes encode transcription factors that play key roles in plant growth and development. However, the specific *B3* genes involved in the seed development of *Akebia trifoliata* remain unexplored.

Results A total of 72 *AktB3* genes were identified and classified into five subfamilies (ARF, LAV, RAV, HSI, and REM) based on phylogenetic analysis. These 72 *AktB3* genes were unevenly distributed across 16 chromosomes. Collinear analysis indicated that segmental duplication has played a significant role in the evolution of *AktB3* genes, and underwent purification selection. Expression profiling across seed development stages revealed that seven *AktB3* genes, particularly from the LAV subfamily (*AktABI3*, *AktFUS3*, *AktLEC2*), were up-regulated at 70 days after flowering (DAF). Notably, the expression of *oleosin* exhibited a strong positive correlation with LAV subfamily genes, highlighting their potential roles as hub genes in lipid metabolism and seed development. Yeast two-hybrid (Y2H) and yeast one-hybrid (Y1H) experiments confirmed that AktFUS3-1, AktFUS3-2, and AktLEC2 form protein complexes and individually bind to the *AktOLE1* promoter, thereby regulating downstream gene expression. These results provide direct evidence of the cooperative role these transcription factors play in controlling lipid metabolism, particularly related to oleosin proteins. Additionally, miRNA sequencing across three seed developmental stages identified 591 miRNAs and 1,673 target gene pairs. A total of 23 *AktB3* genes were predicted to be targets of 20 miRNAs, with 11 miRNAs specifically targeting the ARF subfamily genes. Particularly, miR160-x, miR160-z, and miR167-z were predicted to target ARF subfamily genes, potentially influencing seed development. Moreover, the miRNA-B3 regulatory modules, especially involving *ARF* genes and miR160/167, require further study to clarify their roles in seed development.

Conclusions These findings contribute valuable resources for future functional studies of the molecular regulatory networks governing seed development in *A. trifoliata*.

Keywords *Akebia Trifoliata*, B3 transcription factor, Evolutionary tree, Seed development, MiRNA

Background

Akebia trifoliata (Thunb.) Koidz. (family *Akebia* Decne.) is rich in oil and has various significant medicinal properties [1]. The fruit turns purple upon ripening, has a sweet taste, and is rich in nutrients. It also has a diverse array of bioactive compounds, including saponins and oleanolic acid, and antibacterial, anti-inflammatory, antioxidant, and anticancer properties [2, 3]. *Akebia trifoliata* (abbreviated as *A. trifoliata*) seeds have received increased attention from oil crop researchers because of their high

*Correspondence:
Zhi Zhao
zzhao@gzu.edu.cn
[1] College of Life Sciences, Guizhou University, Guiyang 550025, China
[2] Guizhou Key Laboratory of Propagation and Cultivation of Medicinal Plants, Guizhou University, Guiyang 550025, China

oil content (48.8%) [4]. The oil is rich in vitamins that provide various human health benefits; it is also a raw material for both food and various industrial oils. Chemical analysis of Akebia trifoliata seed oil has revealed that 77.832% and 22.169% of the fatty acids are unsaturated and saturated, respectively [5]. The fatty acid composition, especially the high proportions of oleic acid (42.4%), palmitic acid (21.7%), and linoleic acid (30.5%), contributes to its nutritional value and significant potential for industrial applications [6].

The development of seeds is controlled by a complex regulatory network in which transcription factors play a crucial role. The B3 superfamily of genes is a plant-specific transcription factor family that includes several major gene families, such as LAV (LEAFY COTYLEDON2 [LEC2]-ABSCISIC ACID INSENSITIVE3 [ABI3] - VAL), ARF (AUXIN RESPONSE FACTOR), RAV (RELATED TO ABI3 and VP1), and REM (REPRODUCTIVE MERISTEM) [7–9]. These transcription factors possess a B3 domain, which consists of 110 amino acids and is derived from the third basic domain found in the *VIVIPAROUS1* (*VP1*) gene in maize [10]. Members of the B3 superfamily are widely expressed in plants and have DNA-binding activity [11]. In Arabidopsis and rice, the LAV family can be further divided into the LEC2-ABI3 subgroup and the VAL subgroup [12]. The LEC2-ABI3 subgroup comprises *LEC2*, *ABI3*, and *FUSCA3* (*FUS3*), while the VAL subgroup includes *VAL1*, *VAL2*, and *VAL3*, also known as *HSI2* (HIGH-LEVEL EXPRESSION OF SUGAR-INDUCIBLE GENE 2), *HSL1* (HSI2- LIKE 1), and *HSL2* (HSI2-LIKE2), respectively [13].

The B3 transcription factor plays a vital role in the development and metabolic regulation of plant seeds. In particular, members of the LAV family, including *LEC1*, *LEC2*, *FUS3*, and *ABI3*, play a key role in different stages of seed development. *LEC1* and *LEC2* primarily contribute to maintaining embryogenesis and early cotyledon formation [14, 15], while *FUS3* plays a critical role in regulating the storage of reserves in different regions of the embryo [16]. These genes, along with *ABI3*, collectively regulate the maturation process during the late stages of embryonic development [15, 17]. Moreover, *LEC1* and *FUS3* are essential in the regulation of lipid synthesis. Overexpression of *LEC1* can upregulate genes involved in glycolysis and lipid accumulation, significantly increasing fatty acid and lipid content in transgenic plants [18]. *FUS3* can rapidly induce the expression of fatty acid biosynthesis genes, thereby regulating lipid content in seeds [19]. Auxin response factors play a critical role in regulating plant metabolism. For instance, studies have shown that *SlARF4*, an auxin response factor, is essential for controlling sugar metabolism during tomato fruit development [20]. Downregulation of *SlARF4* not only results in a dark green phenotype and increased chloroplast number in fruits but also leads to starch accumulation and enhanced photosynthetic efficiency at early stages of fruit development. Similarly, overexpression of *SlARF6A* in tomatoes increases chlorophyll content in fruits and leaves, enhances photosynthesis rates, and boosts the accumulation of soluble sugars and starch, whereas downregulation of *SlARF6A* produces opposite phenotypes [21]. In addition, *ARF3* and *ARF6* in bamboo directly regulate lignin biosynthesis genes, influencing lignin synthesis in bamboo [22]. In *Nicotiana tabacum* L., overexpression of *NtARF6* inhibits nicotine biosynthesis [23].

MicroRNAs (miRNAs), a class of non-coding RNA molecules, regulate gene expression by binding to complementary target mRNA sequences [24, 25]. miRNAs play a key role in regulating diverse physiological processes across various plant organs, including roots [26], stems [27], leaves [28, 29], flowers [29], and seeds [30]. Studies have demonstrated that specific miRNAs can regulate seed size, shape, and development by precisely targeting and regulating genes involved in plant hormone signaling pathways, including auxin, gibberellin, and brassinolide [31, 32]. For example, certain miRNAs target auxin-responsive factors to regulate embryonic differentiation and seed formation [33]. Besides directly affecting seed size and morphology, previous studies have also shown that miRNAs influence lipid accumulation by regulating the expression of key genes in plant metabolic pathways, such as lipid metabolism pathways. For example, in Arabidopsis, miRNA159 has been identified to target genes involved in the biosynthesis of lipids, which affects the seed oil content [34]. miRNAs play a key role in the embryogenesis of sea buckthorn seeds and promote efficient oil accumulation [35]. The overexpression of miR5179 in oil palm results in the down-regulation of *NDT1* (NAD transporter 1) expression, which promotes lipid accumulation in oil palm seeds [36]. Additionally, miRNAs and their target genes play significant roles in regulating plant growth and development, responding to environmental stress, and synthesizing metabolites. In Arabidopsis, the miR160-*ARF10/16/17* module plays a crucial role in the interaction between auxin, light, gibberellins (GA), and brassinosteroids (BR) during hypocotyl elongation [37]. In rice, reduced expression of *ARF18* leads to decreased seed set, seed width, and weight, as well as significantly reduced starch accumulation [38]. Moreover, miR160 is closely associated with plant responses to various stress conditions. Overexpression of miR160 increases cotton's sensitivity to heat stress, lowers *ARF10/17* mRNA levels, by activating the auxin response that leads to anther indehiscence [39]. miRNAs also play critical roles in metabolite regulation.

Overexpression of miR160a, by targeting *ARF10/16/17*, reduces GH3-like gene levels in *Salvia miltiorrhiza* hairy roots, thereby negatively regulating tanshinone biosynthesis [40]. The miR160-*ARF10/16* pathway also regulates the biosynthesis of terpene indole alkaloids [41]. Studies have shown that miR160h-*ARF18* may regulate anthocyanin accumulation in poplar [42].

B3 transcription factors have been identified in various plant species, including *Arabidopsis* [7], rice [7], castor [43], olive [44], apricot [45], soybean [46], hemp [47], and pineapple [48]. However, whole-genome analyses of B3 superfamily genes in *A. trifoliata* are lacking. In recent years, advancements in high-throughput sequencing technology have made whole-genome analysis a powerful tool for studying plant gene function and regulatory networks. Identification of B3 gene family members through whole-genome analysis can provide insights into the composition and diversity of this gene family in *A. trifoliata*. Additionally, miRNAs are key regulators of gene expression in plants that bind specifically to target mRNAs to alter their stability and translation efficiency. Therefore, by identifying the members of the *B3* gene family and their roles in seed development and metabolite synthesis, as well as the targeting regulatory effects of miRNAs on *AktB3* genes, we can enhance our understanding of the regulatory mechanisms governing the expression of this gene family.

Results

Identification and phylogenetic analysis of *AktB3* genes

A total of 72 B3 candidate genes were identified in the genome of *A. trifoliata* via hmmsearch and SMART analysis (Supplementary Table S1), and these were referred to as *AktARF1–AktARF27*, *AktREM1_ AktREM26*, *AktHSI1-AktHSI5*, *AktLAV1-AktLAV4* and *AktRAV1- AktRAV10* according to their respective subgroups. The length of these 72 B3 proteins ranged from 145 (*AktRAV6*) to 1,154 (*AktARF24*) amino acid residues, and their molecular weights ranged from 16,342.6 Da (*AktRAV6*) to 129,032.65 Da (*AktARF24*). All the predicted B3 proteins were hydrophilic with isoelectric point values ranging from 5.22 to 9.67. Subcellular localization prediction indicated that most of these proteins were localized to the nucleus (66), and a smaller fraction was located in the cytoplasm (5) and chloroplasts (1).

The evolutionary relationships among AktB3 proteins were investigated by constructing a phylogenetic tree using 72 AktB3 and 118 B3 proteins from Arabidopsis. Five distinct subfamilies (REM, ARF, LAV, HSI, and RAV) of 72 B3 proteins were identified (Fig. 1). Among these subfamilies, the ARF branch had the highest number of genes (27 members), followed by REM (26), LAV (4), HSI (5), and RAV (10).

Analysis of the structure and conserved motifs of *AktB3* genes

We conducted a comprehensive analysis of the structure of *AktB3* genes and found that the 72 *AktB3* genes were classified into five distinct subclasses (Fig. 2A). Approximately 81% of ARF subclass members had between 11 and 15 exons, and RAV subclass members had between 1 and 2 exons. HSI subclass members had 12 to 13 exons, and REM subclass members had 1 to 8 exons. LAV subclass members had 6 exons. A total of 38 AktB3s had both upstream 5'-UTRs and downstream 3'-UTRs. We also identified 10 motifs within these AktB3 sequences; motif 1 and motif 2 were highly conserved B3 domains across all analyzed sequences. The presence of B3 domains was consistently observed in all AktB3s, and high similarity was observed among motifs within subclasses. Specifically, ARF subfamily members had motif 1, along with motifs 2, 3, 5, 7, 8, and 10. Similarly for the HSI, LAV, and RAV gene subsets, motif 2 and motif 7 were present in addition to unique motifs specific to each subclass. Furthermore, the majority of REM members exhibit multiple motif 2, whereas *AktREM24* displays five motif 2.

Multiple sequence alignment of the conserved domains of AktB3 was performed, and genes within the same subclass had similar domains (Supplementary Table S2). Analysis of conserved domains demonstrated that the AktB3 domain comprised seven β chains (β1–β7), with two short α-helices located between β chains 2 and 3 as well as between β chains 5 and 6 (Fig. 2B). Additionally, AktB3 encompasses key DNA contact regions R1–R3 (Fig. 2B). Most amino acid residues were highly conserved in the RAV, ARF, HSI, and LAV subclasses; however, significant variability in amino acid residues was observed in REM members.

Chromosomal localization and gene duplication analysis of *AktB3* genes

AktB3 genes were unevenly distributed across 16 chromosomes (Chr01–Chr16) (Fig. 3). Chromosome 6 had the highest number of *AktB3* genes (10 genes), followed by chromosomes 3 and 4, which each had nine *AktB3* genes. Additionally, chromosomes 2, 8, 11, 12, 13, 14, and 16 had two *AktB3* genes.

We identified collinearity and potential replication events of *AktB3* genes using the MCScanX method. A total of 28 pairs of large replicated fragments were identified, and AktB3 collinearity blocks were located on 16 chromosomes (Fig. 4). The evolutionary history of the *AktB3* genes was assessed by evaluating Ka (nonsynonymous) and Ks (synonymous) values. We calculated Ka/Ks values for 28 pairs of *AktB3* genes, all of which were

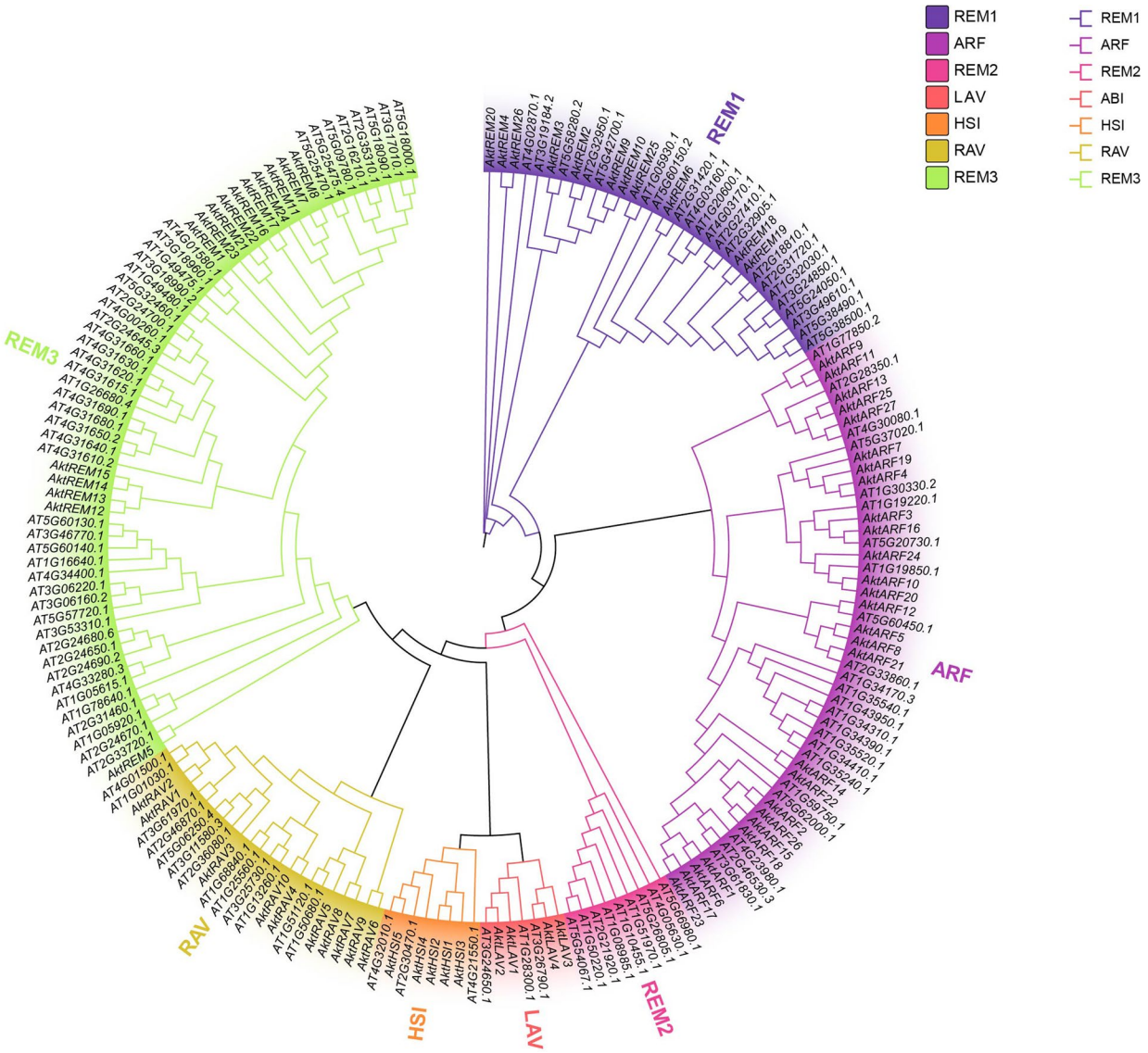

Fig. 1 Phylogenetic analysis of B3 superfamily members in *A. trifoliata* (Akt) and *Arabidopsis thaliana* (AT). A total of 115 members from AT and 72 members from *Akt* were used for phylogenetic analysis. Areas with different colors correspond to different subfamilies

less than 1 (Supplementary Table S3), indicating that they have experienced purifying selection.

We identified 45 collinear gene pairs in *A. trifoliata* and *A. thaliana*, and the most collinear blocks were identified in the *A. trifoliata* chromosomes Chr03/Chr05 and *A. thaliana* chromosomes AtChr01/AtChr02/AtChr03 (Fig. 5, Supplementary Table S4). A total of 30 collinear gene pairs in *A. trifoliata* and rice were revealed. In *A. trifoliata*, the collinear blocks were predominantly located on chromosomes Chr03/Chr09/Chr10/Chr14; in rice, they were mainly found on OsChr01/OsChr04/OsChr06/OsChr07/OsChr11. No collinear blocks were observed on chromosome OsChr12. A total of 22 collinear gene pairs in *A. trifoliata* and grape were identified, and these were primarily located in Chr01/Chr03/Chr04/Chr10 in *A. trifoliata* and VvChr01/VvChr03/VvChr06/VvChr07/VvChr08/VvChr010/VvChr015/VvChr018 in grape. No collinear blocks were observed in VvChr04/VvChr05/VvChr09/VvCh12r16. The number of collinear gene pairs was highest in Arabidopsis B3, indicating a close genetic relationship.

Cis-acting element analysis of *AktB3* gene

An analysis of the cis-acting element of AktB3s revealed numerous CAAT-box and TATA-box elements, as well as elements involved in the response to phytohormones,

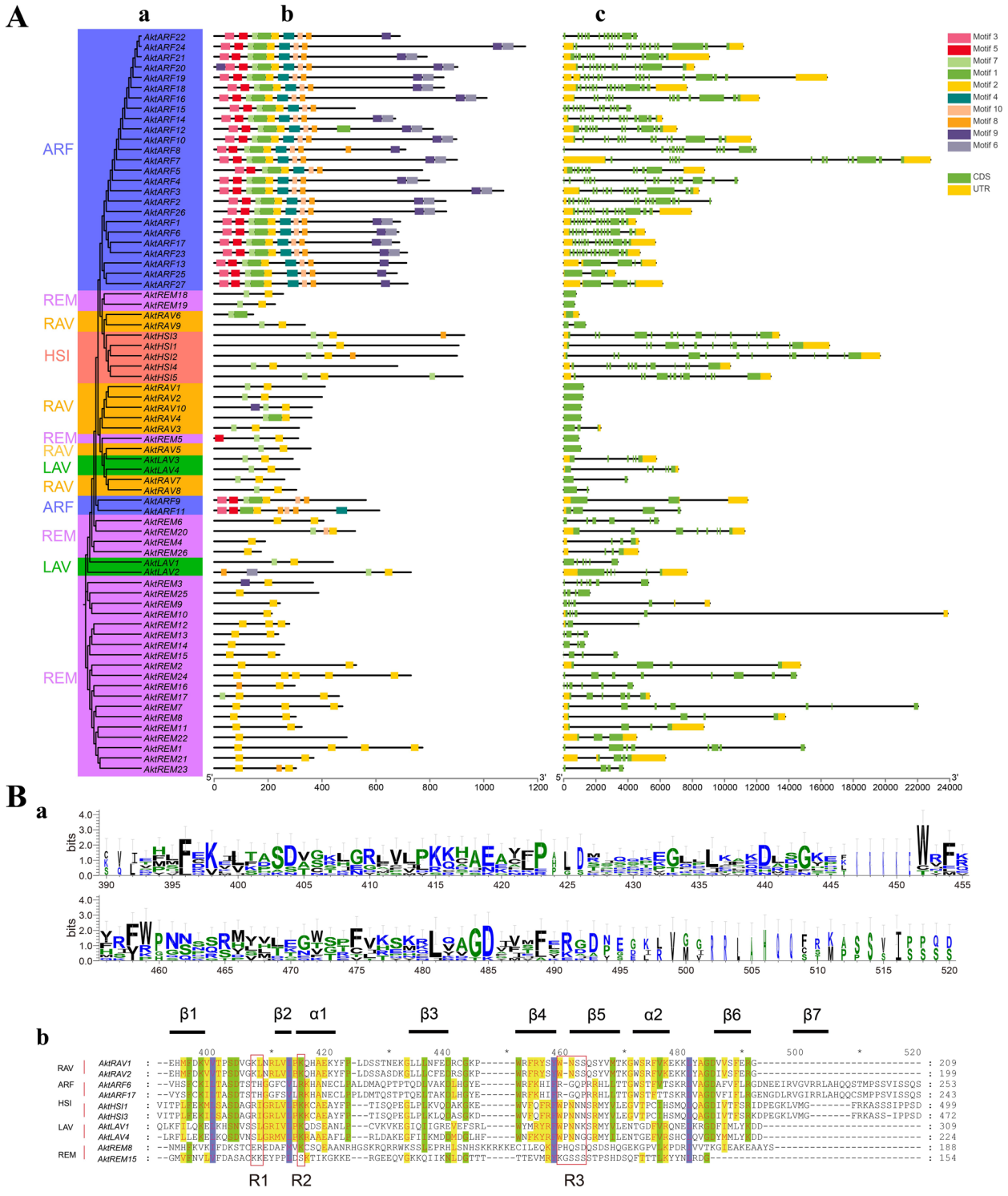

Fig. 2 Phylogenetic relationships, protein structure, gene structure, and conserved domains of the AktB3 superfamily. **A** Fig. 2A(a) shows the adjacency tree constructed from the ARF, LAV, RAV, HSI, and REM subfamilies. Figure 2A (b) shows the structure of B3 proteins, with colors representing motifs. Figure 2A(c) shows the structure of B3 genes, with exons in green, UTR regions in yellow, and black solid lines between colors representing introns. **B** Fig. 2B(a) shows the positions of amino acids on the x-axis and the frequency of each amino acid at a specific position on the y-axis. Different colors are used to represent different types of amino acids. Figure 2B(b) shows the analysis of the conservation of AktB3 amino acid residues. The depth of color indicates the degree of conservation. Darker colors correspond to more conserved amino acids or nucleotides at that position in the sequence

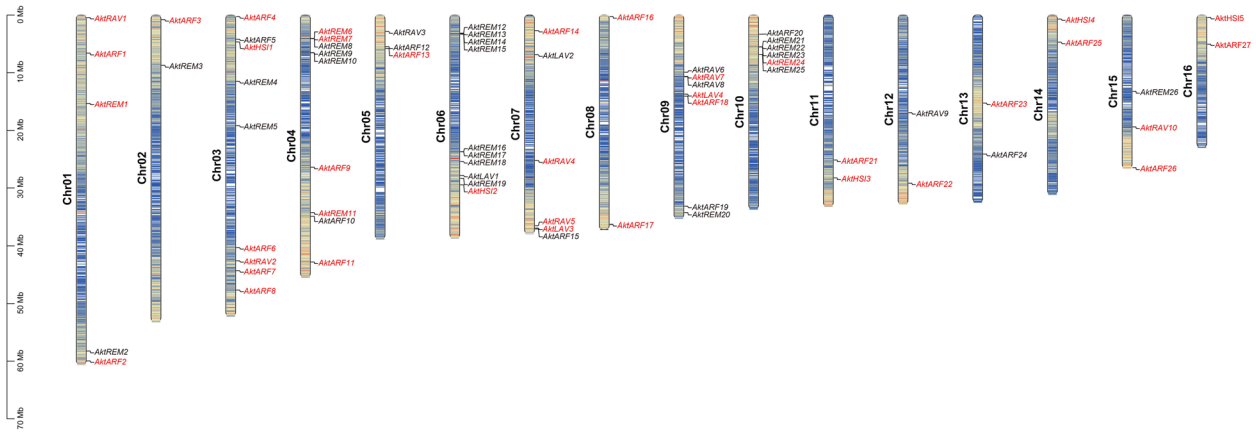

Fig. 3 Chromosomal localization analysis of AktB3 superfamily members. Chr indicates the chromosome number. Red indicates segmentally duplicated genes. Perl 5, version 18, subversion 4 (v 5.18.4) was used for plotting

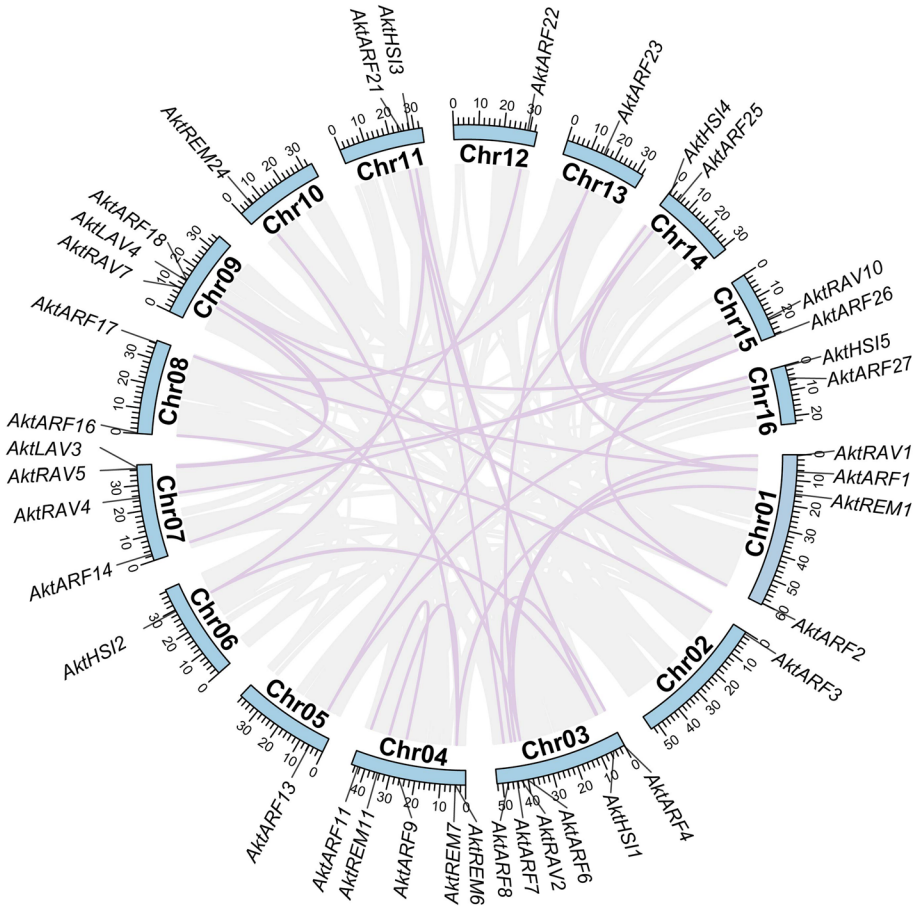

Fig. 4 Collinearity analysis of *AktB3* genes. The purple lines indicate collinear pairs of AktB3

plant growth and development, and abiotic stress (Fig. 6). Twelve elements were identified within the phytohormone response category, and the number of abscisic acid (ABRE), auxin (AuxRR-core, TGA-element), salicylic acid (TCA-element), and methyl jasmonate (CGTCA-motif, TGACG-motif) responsive elements was 286, 15, 59, and 328, respectively. In the plant growth and development category, nine elements were identified. The

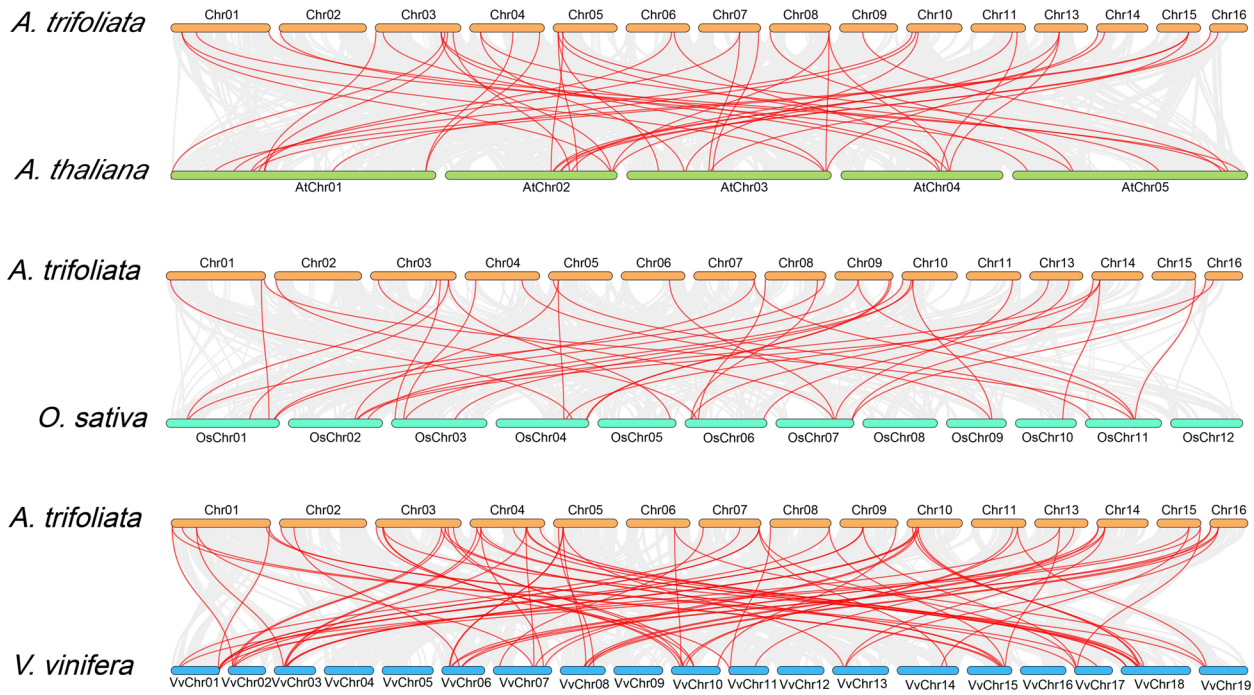

Fig. 5 Collinearity analysis of AktB3 and B3 superfamily members in *A. trifoliata*, *A. thaliana*, *O. sativa*, and *V. vinifera*. Gray lines indicate all pairs of replicated fragments. Red lines indicate pairs of replicated AktB3 fragments

number of elements associated with endosperm expression (GCN4_motif), protein metabolism (O2-site), and phloem expression (CAT-box), seed-specific AT-rich sequences, and RY-elements was 46, 72, 28, 5, and 5, respectively. Additionally, 29 abiotic stress-responsive elements were identified, and these were predominantly Box 4 and G-box elements.

Expression analysis of *AktB3* genes during seed development

To investigate the expression patterns of *AktB3* genes during seed development, transcriptome analyses were performed on seeds from three developmental stages (30 DAF, 50 DAF, and 70 DAF) (Fig. 7A, Supplementary Table S5). According to the transcriptome data, 29 differentially expressed *AktB3* genes were identified; the expression of seven (*AktRAV3*, *AktLAV1*, *AktARF14*, *AktLAV2*, *AktLAV3*, *AktLAV4*, and *AktARF22*) was significantly up-regulated, and the expression of 22 (*AktARF1*, *AktREM1*, *AktARF3*, *AktREM3*, *AktREM4*, *AktREM5*, *AktARF8*, *AktREM6*, *AktREM7*, *AktREM10*, *AktARF10*, *AktARF12*, *AktARF13*, *AktREM12*, *AktREM16*, *AktREM17*, *AktARF15*, *AktARF17*, *AktREM23*, *AktREM25*, *AktARF21*, and *AktARF24*) was significantly down-regulated (Fig. 7A). The expression of *AktLAV2* was highest at 70 DAF, and the expression of *AktARF15* peaked at 30 DAF (Fig. 7A). Fifteen *AktB3* genes were selected to validate the transcriptome data using reverse transcription quantitative PCR (RT-qPCR), which indicated that the expression patterns inferred from qRT-PCR and RNA-seq were consistent (Fig. 7B).

Co-expression network of LAV family members and genes related to lipid synthesis

The LAV family members (*LEC2*, *ABI3*, and *FUS3*) play a crucial role in regulating lipid synthesis [19, 49]. The aim of this analysis is to investigate the regulatory relationships between the LAV family genes—*AktLAV1* (also named *AktLEC2*), *AktLAV2* (also named *AktABI3*), *AktLAV3* (also named *AktFUS3-1*), and *AktLAV4* (also named *AktFUS3-2*)—and lipid synthesis-related genes during seed development. Within our seed RNA-seq database, 66 lipid-related genes were identified across three developmental stages. At 50 DAF, the expression of 17 of these genes was up-regulated; at 70 DAF, the expression of 14 of these genes was up-regulated (Fig. 8A). The expression levels of LAV subfamily genes were high at both 50 DAF and 70 DAF (Fig. 7). A co-expression network was constructed for LAV subfamily and lipid-related genes with Pearson correlation coefficients greater than 0.9 (Fig. 8B, Supplementary Table S6). All four LAV subfamily genes were included in the co-expression network. The five genes with the highest expression at 70 DAF—*mikado.Chr08G1103* (OLE16), *mikado.Chr12G81* (*SAD*), *mikado.Chr16G803*

Fig. 6 Prediction of *cis*-acting elements in the *AktB3* promoter sequences before ATG start codon, which was 2.0 kb

(*FAD2*), *mikado.Chr03G1790* (*PDH*), and *MSTRG.8619* (*ACCase*)—were prominent in the network. These results indicate that LAV family members are closely associated with lipid synthesis genes during key stages of seed development. This co-expression network lays a foundation for further functional studies and helps clarify the specific roles of LAV family members in lipid metabolism.

The interaction between the AktFUS3, AktLEC2, and the *AktOLE1* promoter

We conducted yeast experiments to investigate the interactions between the transcription factors AktFUS3-1, AktFUS3-2, and AktLEC2 with the promoter of the *AktOLE1* gene in *Akebia trifoliata* (Fig. 9). The yeast two-hybrid results showed that all combinations grew normally on SD-LW plates, indicating successful plasmid

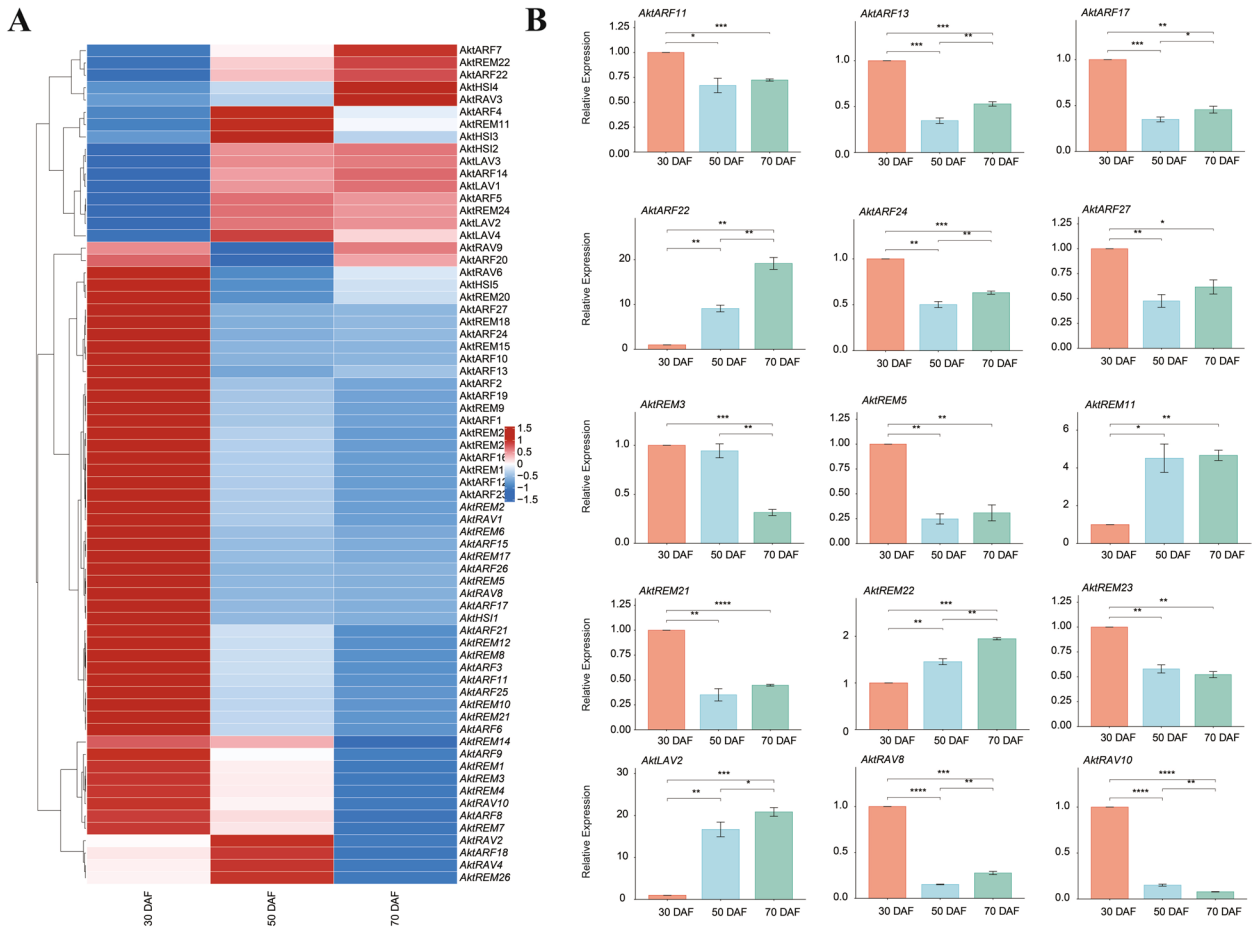

Fig. 7 Expression of *AktB3* genes and qRT-PCR validation during seed development. **A** Heatmap of *AktB3* genes expression based on FPKM values. **B** qRT-PCR validation of the expression patterns of 15 *AktB3* genes. Error bars indicate standard errors (SE) based on three replicates. **P* < 0.05; ***P* < 0.01, Student's *t*-test

transformation (Fig. 9A). The pGADT7 + AktFUS3-1-pGBKT7 and pGADT7 + AktFUS3-2-pGBKT7 transformants did not grow on SD-ALWH or SD-ALWH + x-α-gal plates, indicating that neither AktFUS3-1 nor AktFUS3-2 exhibited self-activation (Fig. 9A). In the experimental group, the AktLEC2-pGADT7 + AktFUS3-1-pGBKT7 and AktLEC2-pGADT7 + AktFUS3-2-pGBKT7 transformants grew normally on SD-ALWH plates and turned blue on SD-ALWH + x-α-gal plates, confirming interactions between AktLEC2 and both AktFUS3-1 and AktFUS3-2 (Fig. 9A).

The yeast one-hybrid results showed that all Y187 strains co-transformed with pHIS2 and pGADT7 plasmids grew successfully on SD-LW plates, indicating successful transformation (Fig. 9B). In the self-activation test, the pGADT7 + *AktOLE1-1*-pHIS2 transformants showed inhibited growth on SD-LWH plates containing 30 mM 3AT, indicating no self-activation (Fig. 9B). Interaction tests showed that the AktFUS3-1-AD/*AktOLE1-1*-pHIS2, AktFUS3-2-AD/*AktOLE1-1*-pHIS2, and AktLEC2-AD/*AktOLE1-1*-pHIS2 transformants all grew normally on SD-LWH plates containing 30 mM 3AT, indicating interactions between these pairs (Fig. 9B). The positive control (pGAD-53/pHIS2-p53) grew normally on 3AT plates, as it could activate the HIS3 reporter gene, while the negative control, unable to activate HIS3, showed inhibited growth on the same plates (Fig. 9B). Therefore, the experiment demonstrated that AktFUS3-1, AktFUS3-2, and AktLEC2 interact with the *AktOLE1-1* promoter in the yeast system.

Identification and analysis of miRNAs targeting *AktB3* genes during seed development

Considering the potential regulatory role of miRNAs in gene expression, particularly in lipid metabolism and seed development, we analyzed the miRNA expression profile associated with AktB3 to further elucidate its regulatory network and contribution to seed development

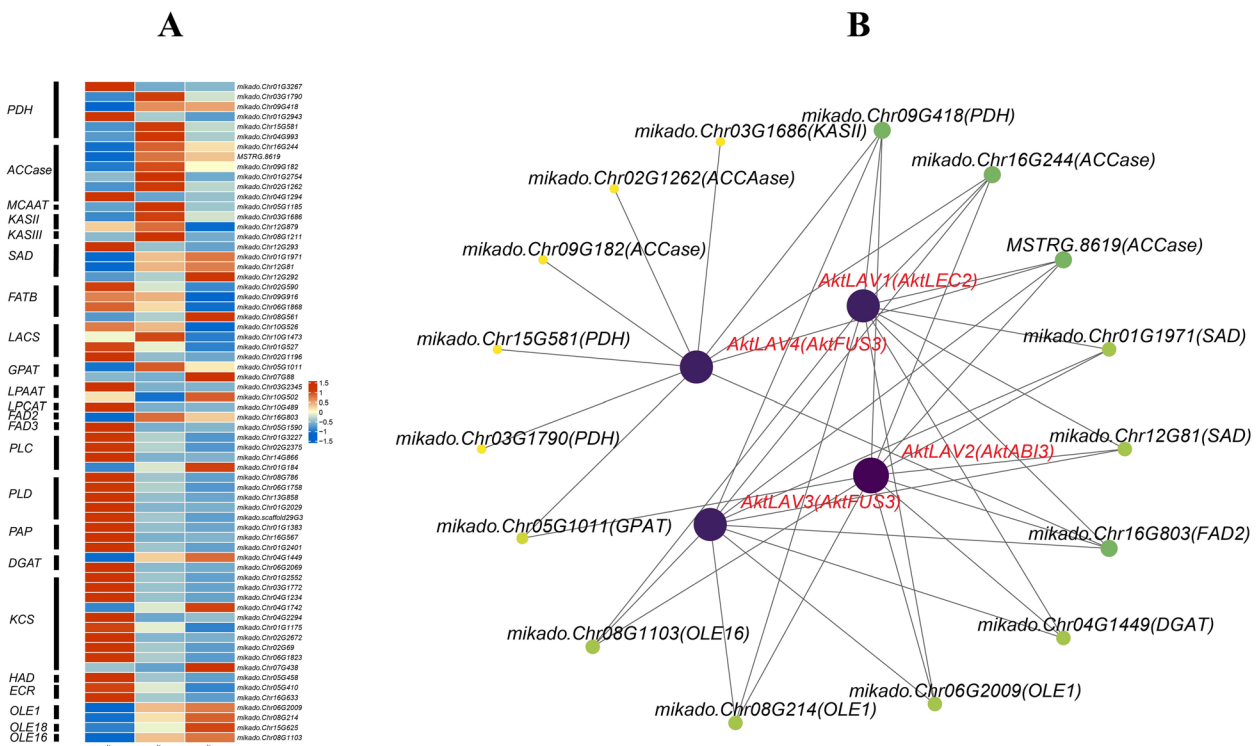

Fig. 8 Co-expression network of AktB3 superfamily genes and genes related to the lipid synthesis pathway. **A** Expression heatmap based on FPKM for genes related to lipid synthesis identified by RNA-seq. **B** Co-expression network of AktB3 and genes related to lipid synthesis with Pearson correlation coefficients greater than 0.9

[50, 51]. To enhance our understanding of miRNA libraries at various stages of seed development, miRNA sequencing was performed on nine seed samples across three developmental stages (30 DAF, 50 DAF, and 70 DAF), and three biological replicates were performed for each sample. Quality and yield assessments of the constructed libraries were conducted using the Agilent 2100 and ABI StepOnePlus Real-Time PCR System (Life Technologies) prior to sequencing. Following the removal of adapters and low-quality reads, a total of 152,401,986 clean reads were generated, which yielded 139,680,762 (91.53%) high-quality clean tags for subsequent analysis (Supplementary Table S7). The distribution of clean tag lengths is shown in Supplementary Table S7. The number of 24-bp tags was 54,816,191 (39.24%), and the number of 21-bp tags was 30,144,959 (21.58%). A total of 591 miRNAs were identified, including 308 known and 283 new miRNAs (Supplementary Table S7).

A total of 1,673 target gene pairs were identified by predictive analyses of target genes for all miRNAs. A total of 23 AktB3 genes were potential targets for 20 miRNAs (Fig. 10A, Supplementary Table S8). The ARF subfamily was targeted by 11 miRNAs, including miR159-x, miR160-x, miR160-z, miR167-z, miR1854-x, miR5234-z, miR5262-z, miR8029-z as well as novel-m0115-5p, novel-m0159-3p and novel-m0228-5p. The REM subfamily was targeted by 5 miRNAs: miR3509-y, miR5290-z, miR6196-z, miR8029-z and miR9751-z. The HSI subfamily was targeted by miR1873-z and novel-m01395p. The RAV subfamily was targeted by miR2931-z and miR5021-z; while the LAV subfamily was targeted by miR1219-z. To identify potential miRNA–mRNA pairs during the development of *A. trifoliata* seeds, miRNAs with TPM values exceeding 1 were selected, and an expression heatmap was constructed. The expression of seven miRNAs (miR167-z, miR5262-z, novel-mo228-5p, miR5021-z, miR9751-z, miR1854-x, and miR159-x) was up-regulated at 70 DAF, and the expression of eight miRNAs (miR160-x, miR160-z, miR6196-z, miR2931-z, miR5234-z, miR5290-z, novel-m0139-5p, and novel-m0159-3p) was down-regulated (Fig. 10B). Pearson correlation coefficients between miRNA and *AktB3* genes expression levels were determined. A total of 26 miRNA–mRNA pairs were significantly negatively correlated according to the following criteria: $|r|>0.9$ and $p<0.05$ (Fig. 10C, Supplementary Table S8). Specifically, six ARF subfamily members were significantly

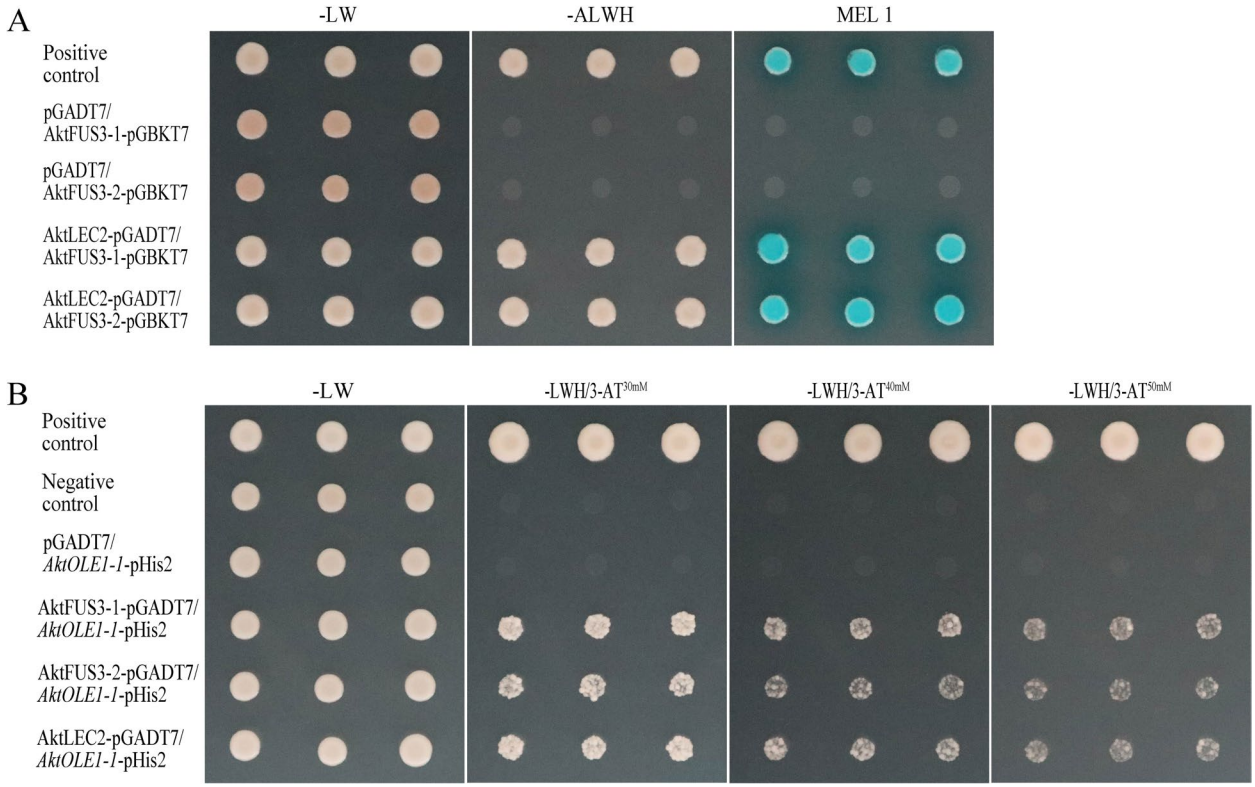

Fig. 9 Yeast two-hybrid and yeast one-hybrid experiments were used to validate the interactions between AktFUS3-1, AktFUS3-2, AktLEC2, and the *AktOLE1* promoter. **A** The yeast two-hybrid assay confirmed the interaction between AktFUS3 and AktLEC2. **B** The yeast one-hybrid assay also validated the interaction between AktFUS3, AktLEC2, and the *AktOLE1* promoter

negatively correlated with miR167-z, miR160-x, and novel-m0228-5p; seven REM subfamily members were significantly negatively correlated with miR167-z and novel-m0228-5p, and two HSI subfamily members were significantly negatively correlated with miR160-z and novel-m0159-3p. Additionally, two LAV subfamily members were negatively correlated with miR160-z. GO functional enrichment analysis of these 26 *AktB3* genes indicated that AktB3 family members might be involved in various biological pathways and processes within plants, including responses to acidic chemicals, reproductive processes, metabolism of nucleotide compounds, transcription of DNA templates, biosynthesis of sesquiterpenes and sesquiterpenoids, metabolism of organic aromatic and nitrogen compounds, and biosynthetic processes (Supplementary Table S8). These genes are likely involved in photoperiodicity, auxin and gibberellin metabolism and biosynthesis, and responses to endogenous and hormonal stimuli. These genes might also regulate processes related to plant growth factor responses (ARF), mediate responses to various stimuli, including sucrose and lipids, and promote embryonic and post-embryonic development, flower development, and vernalization. This indicates that B3 gene family members could play important roles in plant growth, development, and environmental adaptation.

Co-expression network analysis reveals synergistic regulation of seed development and metabolites by miRNAs and *AktB3* genes

By conducting a correlation analysis of 23 miRNAs, 20 *AktB3* genes, and 104 differential abundant metabolites, we constructed a co-expression network (Supplementary Table S9). The results reveal that these miRNAs and AktB3 genes synergistically regulate seed development and various metabolites (Fig. 11A). In this network, miR160-x serves as a central node, capable of regulating the expression of multiple genes, including *AktARF3*, *AktARF11*, *AktREM23*, *AktARF23*, and *AktARF25*. These genes show significant correlations with metabolites such as Hmmp004534 (Hederagenin-O-Hexoside-O-Hexoside-O-Pentoside), Hmmp006650 (saponin A), mws0836 (Procyanidin B1), mws1333 (Melibiose), pmb0854 (LysoPC 18:3), pmb0865 (LysoPC 18:3(2n isomer)), pmb2444 (MAG(18:3)isomer1), pme1210 (L-Methionine), pmn001705 (3,24-Dihydroxy-17,21-semiacetal-12(13)oleanolic fruit) and etc. Additionally, miR160-z regulates *AktHSI1*, *AktREM17*,

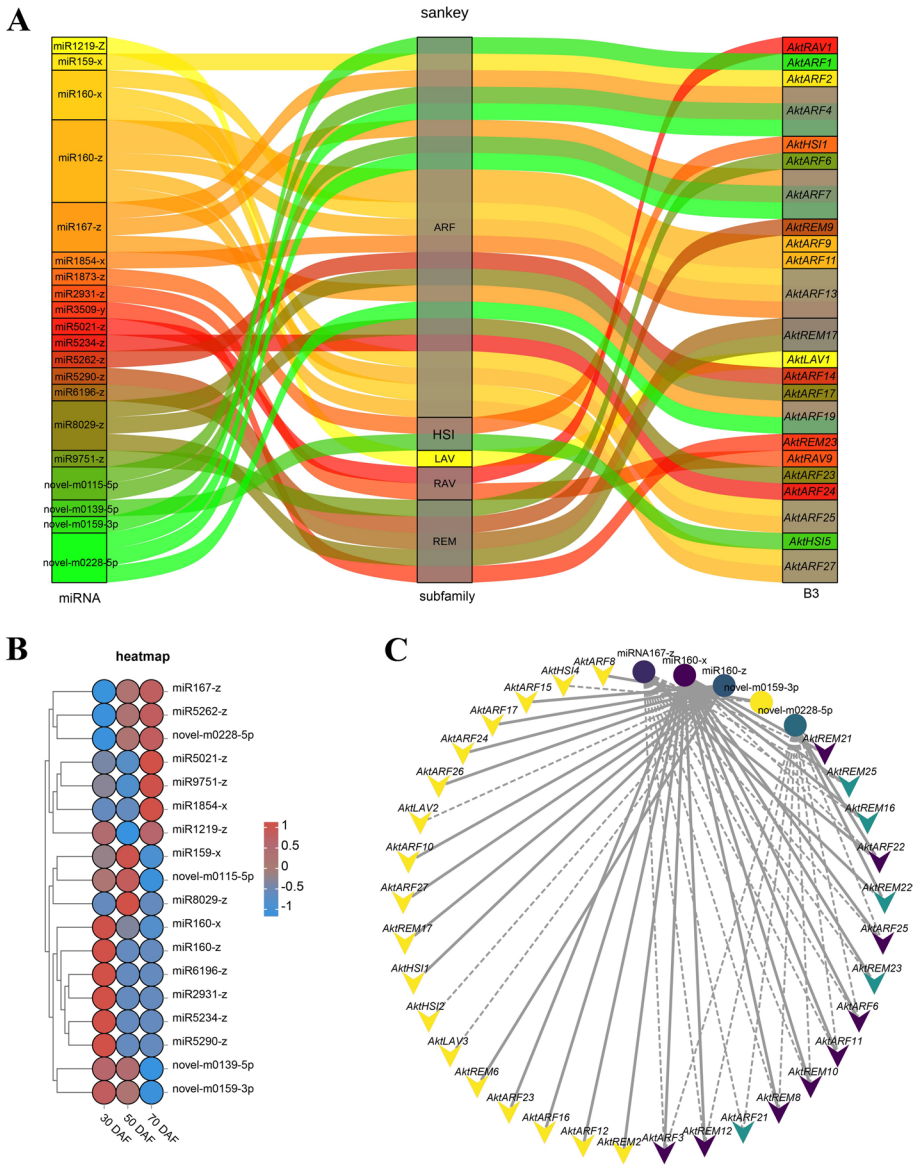

Fig. 10 Identification of miRNAs and targets *AktB3* genes involved in seed development. **A** Prediction of miRNAs targeting *AktB3* genes. A Sankey plot was constructed according to the targeting relationships. **B** The expression heatmap of miRNA targeting *AktB3* genes was plotted using a TPM value > 1. (C) A co-expression network for *AktB3* genes and miRNAs was generated using pairs with $|r| > 0.9$ and $p < 0.05$

AktARF17, *AktARF24*, and *AktARF27*, which are significantly correlated with metabolites such as Hmmp006650 (saponin A), mws0044 (Taxifolin), mws0470, pme0519 (Sucrose), pmp001213 (LysoPC 16:0(2n isomer), and pmb0665 (Luteolin 8-C-hexosyl-O-hexoside). Furthermore, miR167-z regulates *AktARF3*, *AktARF11*, *AktREM23*, and *AktARF25*, showing significant correlations with metabolites like mws0836 (Procyanidin B1), mws1333 (Melibiose), pmb0854 (LysoPC 18:3), pmb2444 (MAG(18:3)isomer1), pmp001213 (Phenylalanine) and etc. These findings provide valuable insights, deepening our understanding of the role of miRNAs in regulating seed development in plants.

To explore the functions of the 20 *AktB3* genes within the co-expression network, we constructed a protein-protein interaction network based on homologous *B3* genes from Arabidopsis. In this network, 13 *AktB3* genes were involved in interactions (Fig. 11B). Notably, 9 *AktB3* genes, along with 14 IAA genes and *ARF9* and *AFB2*, formed the largest subnetwork, with these *AktB3* genes occupying key node positions. Gene Ontology (GO) enrichment analysis predicted a diversity of functions for

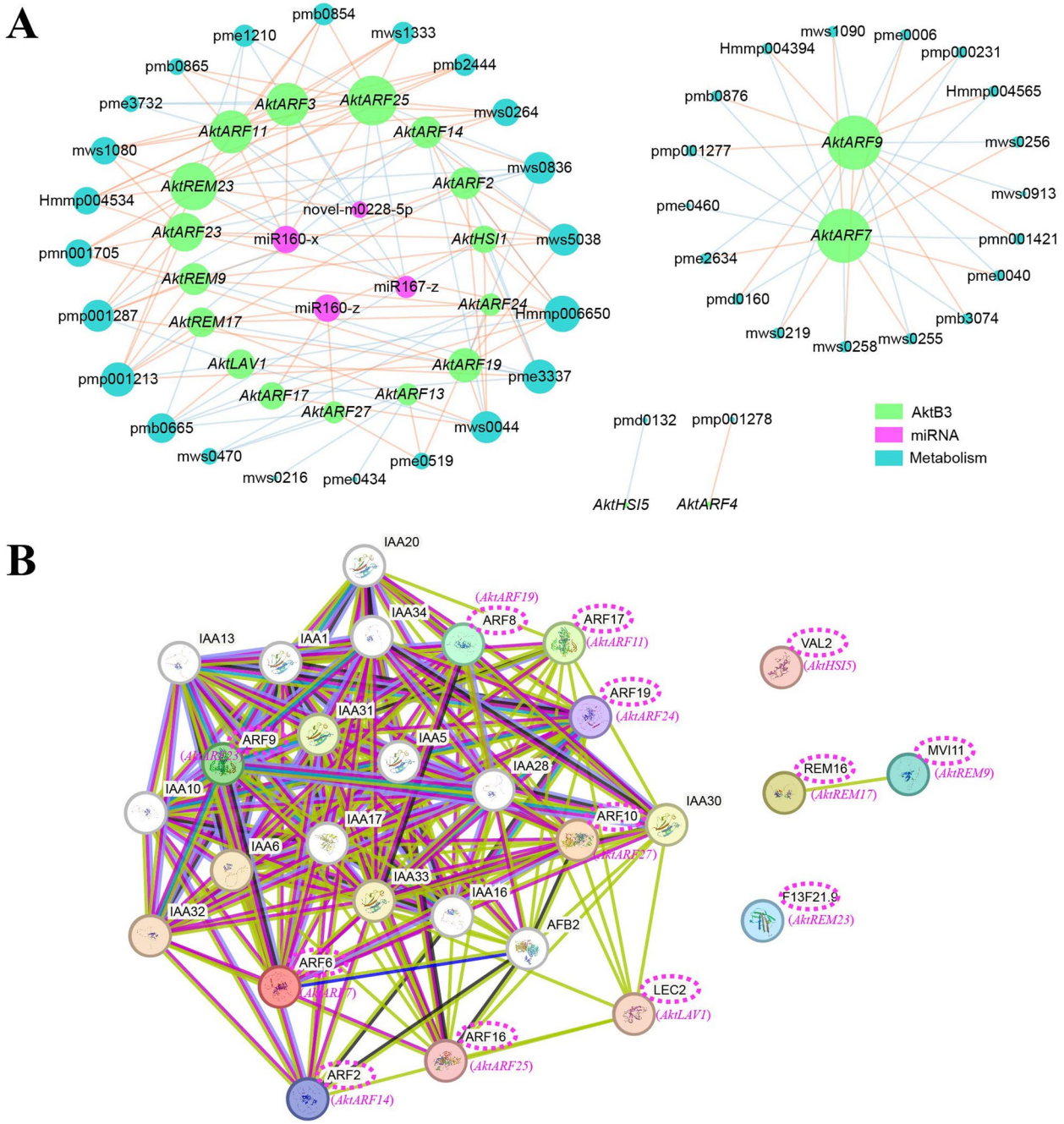

Fig. 11 Co-expression network analysis of *AktB3* genes, miRNA and differential abundant metabolites. **A** A co-expression network analysis for *AktB3* genes, miRNA and differential abundant metabolites was generated using pairs with $|r| > 0.9$ and $p < 0.05$. Yellow lines represent positive correlations, while blue lines represent negative correlations. **B** Protein interaction network analysis of AktB3 proteins in the co-expression network

these genes. The analysis indicated that, in terms of cellular components, these genes are primarily localized in the nucleus. In the function category, they are involved in DNA-binding transcription factor activity, DNA binding, transcription cis-regulatory region binding, sequence-specific DNA binding, identical protein binding, and miRNA binding. In the process category, these genes are implicated in the regulation of cellular processes, system development, multicellular organism development, post-embryonic development, plant organ development, root development, shoot system development, reproductive structure development, fruit development, cellular

processes, flower development, somatic embryogenesis, phyllome development, gravitropism, root cap development, and leaf development (Supplementary Table S10).

Discussion

B3 superfamily members play key regulatory roles in plants, especially in seed development, lipid synthesis pathways, and hormonal signaling during the responses to abiotic stress. In our study, a whole-genome analysis led to the identification of 72 *AktB3* genes. *A. trifoliata* possesses fewer *B3* genes than *Arabidopsis* (118) [7], rice (91) [7], and *Camelina sativa* (87) [52] and more *B3* genes than pineapple (57) [48] and cannabis (65) [47]; the number of *B3* genes in *A. trifoliata* and pecan (75) was similar [53]. Variability in the number of *B3* genes among plant species highlights their diversity and evolution within plant genomes. This variation likely reflects differences in adaptive strategies and the biological features of B3 superfamily genes.

In angiosperms, most ARF, LAV, HSI, and RAV subfamily members are structurally conserved [54]. Our phylogenetic analysis categorized the 72 *AktB3* genes into five subgroups (ARF, REM, LAV, HSI, and RAV), with each containing the characteristic B3 domain. *A. trifoliata* contains 27 ARF members, and 16 contain B3, AUX/IAA, and Aux_resp domains, which suggests that B3 and Aux_resp domains are evolutionarily conserved; this is consistent with the results of a study of pineapple [48]. Four RAV members (*AktRAV10*, *AktRAV4*, *AktRAV5*, *AktRAV8*) also had the AP2 domain. The number of B3 domains in REM and LAV subfamily members ranged from three to five, which indicates that the functional diversity of these subfamilies is high. Phylogenetic analysis revealed structural and sequence similarities among members of different subfamilies. Analysis of introns and exons is important for clarifying the evolution of gene families. More than half of the introns were absent in RAV subfamily genes, and this has also been observed in pecan [53], suggesting that similar selection pressures have resulted in similarity in gene structure in *A. trifoliata* and pecan despite their distinct genetic backgrounds and evolutionary histories. Multiple sequence alignments showed that all *AktB3* genes contain the DNA contact regions R1–R3, and these regions are relatively conserved across the ARF, LAV, HSI, and RAV subfamilies. However, substantial variability in the amino acid residues within the DNA contact regions was observed among REM subfamily members. Similar patterns have been observed in castor bean and Arabidopsis, suggesting that different plant B3 subfamilies might have similar binding specificities [7, 43].

Gene duplication analysis showed that the ARF, HSI, REM, and RAV subfamilies have 18, 3, 3, and 3 duplicated gene pairs, respectively. No gene duplications were detected in the LAV subfamily, and this is consistent with the results of a previous study of grapes [55]. LAV subfamily members are likely highly conserved in trifoliate orange. Collinear gene pairs were identified between *A. trifoliata* and Arabidopsis, rice, and grape (45, 32, and 22, respectively). This suggests that *A. trifoliata* and Arabidopsis B3 members might share a common ancestor; this will facilitate future studies of the evolution and function of B3 genes.

RNA-seq analysis of *A. trifoliata* seeds at various developmental stages revealed that the expression of genes from five ARF, four LAV, two RAV, two HSI, and two REM subfamilies was up-regulated at 70 DAF. *AktARF14* and *AktARF22*, homologs of Arabidopsis *ARF1*, have been demonstrated to significantly affect cell plate formation, Golgi apparatus maintenance, and plant growth in Arabidopsis [56]. *AktARF7*, a homolog of Arabidopsis *ARF8*, is related to *ARF8.1*, an Arabidopsis splice variant that regulates pollen cell wall formation [57]. The *PpIAA5-ARF8* module governs the regulation of peach fruit ripening and softening [58]. In grapes, the expression of RAV and REM in both seedless and seeded varieties indicates that these subfamilies might contribute to seed development or sterility [55].

Four LAV genes in *A. trifoliata—AktLAV1* (homolog of *LEC2*), *AktLAV2* (homolog of *ABI3*), *AktLAV3* (homolog of *FUS3*), and *AktLAV4* (homolog of *FUS3*)—were highly expressed during the rapid lipid accumulation stage of seed development, and they were strongly positively correlated with 16 lipid-related genes. Our studies revealed that *AktLAV1* (*AktLEC2)*, *AktLAV3* (*AktFUS3-1)*, *AktLAV4* (*AktFUS3-2)* and *AktLAV2* (*AktABI3*) are co-expressed with three lipid protein-related genes (*OLE1*, *OLE16*). *ABI3* has been shown to significantly up-regulate oleosin proteins, including OLEOSINS and CALEOSINS, which activates lipid accumulation [59]. *FUS3* mutations result in decreases in the oil content in canola [59]. Two adjacent RY elements are required in the promoter of *LEC2* for OLEOSIN expression to be effectively activated [60]. The yeast two-hybrid experiment indicates that AktFUS3 may form a complex with AktLEC2, working together to regulate the expression of specific genes. The yeast one-hybrid experiment revealed that AktFUS3 can independently bind to specific DNA sequences, either activating or repressing target gene expression. This binding may enhance or modulate regulatory activity through interaction with AktLEC2. As B3-type transcription factors, the interaction between AktFUS3 and AktLEC2 may directly regulate the Oleosin gene (*AktOLE1*) or other lipid metabolism-related genes, affecting oil synthesis and storage in plants.

We developed small RNA libraries for various stages of seed development and performed predictions of miRNA target genes. A total of 34 miRNA-AktB3 target gene pairs were identified, including miRNA-ARF pairs such as miR159-*ARF7*, miR160-*ARF10*, miR160-*ARF16*, miR160-*ARF17*, miR167-*ARF6*, and miR167-*ARF8*. Our studies revealed significant negative correlations of certain ARF subfamily members—*AktARF25* (homolog of *ARF10*), *AktARF6* (homolog of *ARF18*), *AktARF11* (homolog of *ARF17*), *AktARF21* (homolog of *ARF3*), *AktARF3* (homolog of *ARF7*), and *AktARF22* (homolog of *ARF1*)—with miR167-z, miR160-x, and novel-m0228-5p. These findings enhance our understanding of the regulatory interactions within the ARF subfamily during seed development. Previous research has demonstrated that miRNA-mediated auxin response factors—*ARF10*, *ARF16*, and *ARF17*—play key roles in regulating multiple facets of plant growth and development [61]. For example, miRNAs can modulate integument growth by targeting ARFs, and the suppression of miRNA160 leads to reduced seed size in cotton [62]. miR160 is thought to control somatic embryogenesis by targeting *ARF10/ARF16* within the auxin biosynthesis pathway regulated by *LEC2* [63]. The targets of xso-miR160d and xso-miR167a in *Xanthoceras sorbifolium* were identified as *XsARF6* and *XsARF16*, respectively. This microRNA-ARF module may play a crucial role in regulating the development of *Xanthoceras sorbifolium* pistil [64]. miR167 also shows a similar regulatory pattern, targeting *ARF6* and *ARF8*. miR167a, as a maternal effect gene, participates in embryo and seed development. The novel miR167a-*OsARF6-OsAUX3* module regulates grain length and weight in rice [65]. In rice, miR167d influences flower opening and stigma size by regulating *ARF6*, *ARF12*, *ARF17*, and *ARF25* [66]. In *Akebia trifoliata*, miR167 is upregulated at 70 DAF, while its target *ARF* genes are downregulated, indicating that the miR167-ARF6 module might mediate seed size and development. Hence, our research findings demonstrate that miR167-z, miR160-x, and miR160-z can target ARF to regulate normal seed growth and embryo development in *A. trifoliata*.

By constructing a co-expression network, we explored the synergistic regulatory mechanisms between miRNAs and *AktB3* genes, which collectively regulate various metabolites during seed development. In this study, miR160-x, miR160-z, and miR167-z emerged as core regulatory nodes in the co-expression network. These miRNAs directly target specific members of the *AktB3* gene family, such as *AktARF3* (homolog of Arabidopsis *ARF19*), *AktARF11* (homolog of Arabidopsis *ARF17*), *AktARF23* (homolog of Arabidopsis *ARF18*), and *AktARF25* (homolog of Arabidopsis *ARF10*), to regulate their expression. Studies have shown that the miRNA160–*ARF17*–*HYPONASTIC LEAVES 1* module is crucial for drought resistance in apple (*Malus domestica*) [67]. In the somatic embryogenesis of leaf cells, miR160 interacts with *ARF18* target sites to negatively regulate their expression [68]. Therefore, the miR160-ARF17 module in *Akebia trifoliata* is likely associated with drought resistance, while the miR160-ARF18 module may be involved in somatic embryogenesis. Furthermore, the regulatory interactions between miRNAs and *AktB3* genes have a significant impact on related metabolic pathways and biological functions. In this study, specific *AktB3* genes like *AktARF2* (homolog of Arabidopsis *ARF2*) and *AktARF17* (homolog of Arabidopsis *ARF18*) showed a high correlation with compounds like taxifolin and procyanidin B2. Research indicates that *ARF2* acts as a positive regulator, finely tuning the spatial and temporal accumulation of flavonols and proanthocyanidins in Arabidopsis [69]. Moreover, the miR160h-*ARF18* module may also regulate anthocyanin biosynthesis in poplar [42]. Therefore, the miR160-z-*ARF18* module may be involved in the synthesis of procyanidin in *Akebia trifoliata*. In soybean, the miR160a-*GmARF16-GmMYC2* module regulates proline synthesis, reducing damage from osmotic stress and maintaining salt stress tolerance [70]. The increased proline content in *Akebia trifoliata* seeds may be crucially regulated by the miR160-*ARF16* module in response to environmental stress. In summary, miRNAs and their target genes play significant roles in regulating plant growth and development, responding to environmental stresses, and synthesizing metabolites. However, the specific functions and mechanisms of these miRNA-mediated regulatory pathways require further investigation to be fully elucidated.

Conclusions

In this study, we identified 72 members of the B3 superfamily in *Akebia trifoliata* and found that certain genes play pivotal roles in seed development and lipid metabolism. Notably, genes from the LAV subfamily—*AktABI3*, *AktFUS3-1*, *AktFUS3-2*, and *AktLEC2*—emerged as potential hub genes regulating seed oil accumulation, as their expression was highly correlated with key lipid-related genes (*AktOLE1*, *AktOLE16*) during critical stages of seed maturation. Moreover, the Y2H and Y1H experiments confirmed that AktFUS3-1, AktFUS3-2, and AktLEC2 form protein complexes and directly interact with the *AktOLE1* promoter, regulating downstream gene expression. Additionally, miR160-x, miR160-z, and miR167-z were predicted to target ARF subfamily genes and may play a crucial role in seed development. Further research is needed to explore the regulatory roles of *ARF* genes and the miR160/167 gene modules in seed development to gain a deeper understanding of their functions.

Methods

Plant material

Field surveys and sample collection were carried out from May to July 2019 at the Guizhou University Teaching Experimental Field in Huaxi District, Guiyang City, Guizhou Province (26°41'04.35"N, 106°68'36.51"E). The plant material of *Akebia trifoliata* (Thunb.) koidz. was identified by Prof. Zhao Zhi, who is the corresponding author of this paper and affiliated with Guizhou University. This *Akebia trifoliata* was "mutong No. S1". We collected seeds of *Akebia trifoliata* from the Teaching Experimental Farm of Guizhou University and stored them at a temperature of 4 °C in our laboratory. The trees were marked on the day of full bloom (April 20, 2019). Samples were collected from *A. trifoliata* at three developmental stages: 30 DAF, 50 DAF, and 70 DAF. Fruit peels and pulps were removed, and three biological replicates were performed for each stage. The seed samples were immediately frozen in liquid nitrogen and stored at -80 °C until transcriptomic and small RNA-seq analyses.

Identification of B3 gene family members in *A. trifoliata*

The B3 protein sequences of Arabidopsis were obtained from the Arabidopsis Information Resource (https://plants.ensembl.org/Arabidopsis_thaliana/Info/Index). These sequences were used as queries in the Arabidopsis Genome Database (TAIR, https://www.arabidopsis.org/). The Hidden Markov Model (HMM) matrix for the B3 domain (PF02362) was obtained from Pfam (http://pfam.xfam.org/family0029. B3 gene family members in trifoliate orange were predicted using the hmmsearch tool with the following parameters: --domE 1e-10 –notextw. The NCBI-CDD (https://www.ncbi.nlm.nih.gov/cdd/) and SMART (http://smart.embl-heidelberg.de/) online tools were used to authenticate the B3 genes, identify false positives, and predict the conserved structural domains of the B3 proteins.

Chromosomal localization and duplication analysis of B3 Gene Family members

The chromosomal locations of B3 genes on chromosomes were determined using gene annotation data, and they were mapped using Map Gene2Chromosome V2 (http://mg2c.iask.in/mg2c_v2.0/). Advanced Circos within TBtools was used to perform both intraspecific and interspecific collinearity analyses. The selection pressures acting on the B3 gene family in *A. trifoliata* were identified using PAL2NAL (http://www.bork.embl.de/pal2nal/).

BLAST searches were performed using whole-genome data for *A. trifoliata* obtained from the NGDC (https://ngdc.cncb.ac.cn/; Bioproject: PRJCA012651). Genomic sequences of *Arabidopsis thaliana*, *Oryza sativa*, and *Vitis vinifera* were obtained from Ensembl (https://plants.ensembl.org/index.html). A local BLAST database was established to facilitate comparisons between the *A. trifoliata* genome and these three genomes. Intergenomic collinearity was analyzed using MCScanX, and the results were visualized using TBtools.

Analysis of the structure, phylogenetic relationships, and *cis*-acting elements of B3 gene family members

The basic physicochemical properties of B3 family proteins were analyzed using ExPASy software (https://web.expasy.org/protparam/). The subcellular localization was predicted using WoLF PSORT (https://wolfpsort.hgc.jp/). Multiple sequence alignment of AktB3 and AtB3 proteins was performed using MEGA 7.0. The phylogenetic tree was constructed using the neighbor-joining method with 1,000 bootstrap replicates; other parameters were set to their default values. The phylogenetic tree was visualized using Evolview (https://www.evolgenius.info/evolview/).

Gene structures were delineated and visualized using TBtools (v. 1.0987663) and the Gff annotation file data. Perl scripts were used to extract sequences 2,000-bp upstream from B3 transcription start sites for analysis, and *cis*-acting elements were screened using the tools in PlantCARE (http://bioinformatics.psb.ugent.be/webtools/plantcare/html/).

Transcriptome analysis and qRT-PCR validation of AktB3 genes

Primers for qRT-PCR were designed using Primer 5.0 software. Total RNA was extracted using the cetyltrimethylammonium bromide (CTAB) method, and RG19 (histone h3) was used as the internal reference gene. The iScript™ gDNA Clear cDNA Synthesis Kit was used to generate first-strand cDNA from 16 µL of gDNA on ice; the mixture was incubated at 25 °C for 5 min and 75 °C for 5 min to degrade gDNA. This was followed by the preparation of a 20 µL reverse transcription mix, which was incubated at 25 °C for 5 min, 46 °C for 20 min, and 95 °C for 5 min. qPCR was performed on an ABI QuantStudio 6 Flex Real-Time PCR System using SYBR Premix EX Taq. The reaction mixture included 10 µL of 2× qPCR Mix, 0.5 µL of each primer, 0.5 µL of cDNA, and 8.5 µL of ddH_2O. The amplification protocol was set to 95 °C for 300 s, followed by 40 cycles of 95 °C for 10 s and 60 °C for 30 s. Relative gene expression was calculated using the 2-ΔΔCT method, and 30 DAF served as the reference point.

The yeast two-hybrid assay was used to determine the interaction between AktFUS3 and AktLEC2

AktFUS3-1 and AktFUS3-2 were cloned into the pGBKT7 vector using NdeI and NotI restriction enzymes. Similarly, the gene *AktLEC2* was cloned into the pGADT7 vector using NdeI and XhoI enzymes for subsequent functional studies or protein expression. Competent Y2H gold cells were prepared, and various combinations of pGADT7 and pGBKT7 plasmids were co-transformed into Y2H gold yeast strains, including self-activation control, experimental, positive control, and negative control groups. The transformants were first screened on SD-LW plates (lacking leucine and tryptophan) to confirm successful co-transformation of the plasmids. Colonies were then transferred to SD-ALWH plates (lacking leucine, tryptophan, histidine, and adenine) and SD-ALWH plates supplemented with x-α-gal for further screening and analysis. The expression of the HIS3, ADE2, and MEL1 reporter genes was monitored to assess the growth of the strains and the x-α-gal color reaction, determining the presence of self-activation and interactions.

Yeast one-hybrid assays were used to verify the interactions between AktFUS3-1, AktFUS3-2, AktLEC2, and the *AktOLE1-1* promoter

AktFUS3-1 was cloned into the pGAD-T7 vector using NdeI and XhoI restriction enzymes for subsequent functional studies or protein expression. Similarly, *AktFUS3-2* was cloned into the pGAD-T7 vector using NdeI and BamHI enzymes for the same purposes. The target gene *AktOLE1-1* promoter was cloned into the pHIS2 vector using EcoRI and MluI restriction sites, with ligation performed by T4 DNA ligase. The plasmid was amplified in Top10 cells and selected using kanamycin resistance. The resulting recombinant plasmid containing the target gene *AktOLE1-1* was used for yeast one-hybrid assays. Plasmid combinations (AktFUS3-1-pGADT7/*AktOLE1-1*-pHIS2, AktFUS3-2-pGADT7/*AktOLE1-1*-pHIS2, AktLEC2-pGADT7/*AktOLE1-1*-pHIS2, pGADT7/*AktOLE1-1*-pHis2) were co-transformed into Y187 yeast strains. The transformed yeast cells were cultured in YPDA liquid medium, followed by centrifugation, resuspension, and washing. The transformation was performed using a solution of 50% PEG3350, LiAc, and plasmid DNA. The transformed cells were plated on SD-LW selective media to isolate transformants. Colonies were then transferred to SD-LWH plates with varying concentrations of 3AT (30 mM, 40 mM, and 50 mM) to observe their growth in the presence of 3AT.

Sequencing and identification of snRNAs

After total RNA was extracted using the Trizol reagent kit (Invitrogen, Carlsbad, CA, USA), RNA molecules ranging in size from 18 to 30 nt were enriched by polyacrylamide gel electrophoresis (PAGE). The 3′ adapters were added, and the 36–48 nt RNAs were enriched. The 5′ adapters were then ligated to the RNAs as well. The ligation products were reverse-transcribed by PCR amplification, and PCR products ranging from 140 to 160 bp in size were enriched to generate a cDNA library and sequenced using Illumina HiSeq Xten by Gene Denovo Biotechnology Co. (Guangzhou, China).

All the clean tags were aligned against small RNAs in the GenBank database (Release 209.0) and Rfam database (Release 11.0) to identify and remove rRNAs, scRNAs, snoRNAs, snRNAs, and tRNAs. All the clean tags were also aligned against the reference genome. Those mapped to exons or introns might be fragments derived from mRNA degradation; these tags were thus removed. The tags mapped to repeat sequences were also removed.

Searches of the clean tags against the miRBase database (Release 22) were performed to identify known miRNAs (exist miRNAs). To date, the miRNA sequences of some species are not included in the miRBase database. For these species, the alignment of miRNAs with other species was an effective approach for identifying the known miRNAs. All of the unannotated tags were aligned to the reference genome. The novel miRNA candidates were identified according to their genome positions and hairpin structures predicted by mirdeep2 software.

Functional annotation, small RNA expression profiles, and target prediction

Total miRNA comprised exist miRNA, known miRNA, and novel miRNA based on their expression patterns in each sample, and the miRNA expression level was calculated and normalized to transcripts per million (TPM). Analysis of the differential expression of miRNAs between groups and samples was performed using edgeR software. We identified significant differentially expressed miRNAs using the following criteria: fold change ≥ 2 and P-value < 0.05.

Based on the exist miRNA, known miRNA, and novel miRNA sequences, the candidate target genes were predicted using PatMatch (Version 1.2) software.

miRNA target network analysis and protein-protein interaction network analysis of AktB3

Pearson correlation coefficients (PCC) were used to evaluate the correlations between miRNA and target gene expressions, as well as between target genes and metabolite expressions. Pairs with a PCC greater than

0.9 or less than −0.9 and a p-value less than 0.05 were identified as co-expressed miRNA-target gene pairs. The miRNA-target network was then constructed and visualized using Cytoscape software (v3.6.0). The protein interaction network was constructed using the STRING database (https://cn.string-db.org/). The metabolic data is derived from published articles [71].

Supplementary Information

The online version contains supplementary material available at https://doi.org/10.1186/s12864-024-10981-0.

Supplementary Material 1.
Supplementary Material 2.
Supplementary Material 3.
Supplementary Material 4.
Supplementary Material 5.
Supplementary Material 6.
Supplementary Material 7.
Supplementary Material 8.
Supplementary Material 9.
Supplementary Material 10.

Acknowledgements
The authors thank to all people who provided help for this article.

Authors' contributions
ZZ conceived the study; HL (Hongchang Liu) supervised the study; JL and CX performed the experiments; HL (Huijuan Liu) wrote the manuscript; ZZ provided funding. All authors have read and agreed to the published version of the manuscript.

Funding
This research was funded by the Talent 532 Base Project of Organization Department in Guizhou Province, China (Grant numbers: QRLF (2013) 533 no.15, QRLF (2016) no. 23, and QRLF (2020) no. 2).

Data availability
Whole-genome data are available at the following link: https://bigd.big.ac.cn/gsa/browse/CRA008753, under project ID PRJCA012651 and accession number CRA008753. Transcriptome data were acquired from the NCBI Sequence Read Archive (SRA) under the BioProject ID PRJNA884501. Small RNA data were obtained from the BIG Submission under the project ID PRJCA025482 and accession number CRA016160.

Declarations

Ethics approval and consent to participate
The *Akebia trifoliata* used in this study was cultivated in the Teaching Experimental Farm of Guizhou University, Huaxi District, Guiyang City, Guizhou Province, China. Collection of plant materials complied with the institutional, national and international guidelines. No specific permits were required.

Consent for publication
Not applicable.

Competing interests
The authors declare no competing interests.The *Akebia trifoliata* used in this study was cultivated in the Teaching Experimental Farm of Guizhou University, Huaxi District, Guiyang City, Guizhou Province, China. Collection of plant materials complied with the institutional, national and international guidelines. No specific permits were required.

Received: 26 April 2024 Accepted: 30 October 2024
Published online: 09 November 2024

References

1. Maciąg D, Dobrowolska E, Sharafan M, Ekiert H, Tomczyk M, Szopa AJJE. *Akebia quinata* and *Akebia trifoliata*-a review of phytochemical composition, ethnopharmacological approaches and biological studies. J Ethnopharmacol. 2021;280: 114486. https://doi.org/10.1016/j.jep.2021.114486.
2. Tang ZY, Li Y, Tang YT, Ma XD, Tang ZY. Anticancer activity of oleanolic acid and its derivatives: recent advances in evidence, target profiling and mechanisms of action. Biomed Pharmacother. 2022;145:112397. https://doi.org/10.1016/j.biopha.2021.112397.
3. Choi J, Jung H-J, Lee K-T, Park H-JJJ. Antinociceptive and anti-inflammatory effects of the saponin and sapogenins obtained from the stem of *Akebia quinata*. J Med Food. 2005;8(1):78–85. https://doi.org/10.1089/jmf.2005.8.78.
4. Su S, Wu J, Peng X, Li B, Li Z, Wang W, Ni J, Xu XJJFC. Analysis: genetic and agro-climatic variability in seed fatty acid profiles of *Akebia trifoliata* (Lardizabalaceae) in China. J Food Compos Anal. 2021;102: 104064. https://doi.org/10.1016/j.jfca.2021.104064.
5. Zhong Y, Zhang Z, Chen J, et al. Physicochemical properties, content, composition and partial least squares models of A. trifoliata seeds oil. Food Chem. 2021;12:100131.https://doi.org/10.1016/j.fochx.2021.100131.
6. Zhao S-Q, Hu J-N, Zhu X-M, Bai C-Q, Peng H-L, Xiong H, Hu J-W, Zhao Q. Characteristics and feasibility of Trans-Free Plastic Fats through Lipozyme TL IM-Catalyzed interesterification of Palm Stearin and *Akebia Trifoliata* Variety Australis seed oil. J Agri Food Chem. 2014;62(14):3293–300. https://doi.org/10.1021/jf500267e.
7. Swaminathan K, Peterson K, Jack TJT. The plant B3 superfamily. Trends Plant Sci. 2008;13(12):647–55. https://doi.org/10.1016/j.tplants.2008.09.006.
8. Yamamoto A, Kagaya Y, Usui H, Hobo T, Takeda S, Hattori TJP. Physiology c: diverse roles and mechanisms of gene regulation by the Arabidopsis seed maturation master regulator FUS3 revealed by microarray analysis. Plant Cell Physiol. 2010;51(12):2031–46. https://doi.org/10.1093/pcp/pcq162.
9. Angeles-Núñez JG, Tiessen AJJ. Mutation of the transcription factor LEAFY COTYLEDON 2 alters the chemical composition of Arabidopsis seeds, decreasing oil and protein content, while maintaining high levels of starch and sucrose in mature seeds. J Plant Physiol. 2011;168(16):1891–900. https://doi.org/10.1016/j.jplph.2011.05.003.
10. McCarty DR, Hattori T, Carson CB, Vasil V, Lazar M, Vasil IKJC. The Viviparous-1 developmental gene of maize encodes a novel transcriptional activator. Cell. 1991;66(5):895–905. https://doi.org/10.1016/0092-8674(91)90436-3.
11. Suzuki M, Kao CY, McCarty DR. The conserved B3 domain of VIVIPAROUS1 has a cooperative DNA binding activity. Plant Cell. 1997;9(5):799–807. https://doi.org/10.1105/tpc.9.5.799.
12. Jo L, Pelletier JM, Hsu S-W, Baden R, Goldberg RB, Harada JJJPNAS. Combinatorial interactions of the LEC1 transcription factor specify diverse developmental programs during soybean seed development. Proc Natl Acad Sci U S A. 2020;117(2):1223–32. https://doi.org/10.1073/pnas.1918441117.
13. Tsukagoshi H, Saijo T, Shibata D, Morikami A, Nakamura KJPP. Analysis of a sugar response mutant of Arabidopsis identified a novel B3 domain protein that functions as an active transcriptional repressor. Plant Physiol. 2005;138(2):675–85. https://doi.org/10.1104/pp.104.057752.
14. Ledwoń A, Gaj MD. LEAFY COTYLEDON1, FUSCA3 expression and auxin treatment in relation to somatic embryogenesis induction in Arabidopsis. Plant Growth Regul. 2011;65(1):157–67. https://doi.org/10.1007/s10725-011-9585-y.
15. Nambara E, Keith K, McCourt P, Naito SJD. A regulatory role for the *ABI3* gene in the establishment of embryo maturation in Arabidopsis thaliana. Development. 1995;121(3):629–36. https://doi.org/10.1242/dev.121.3.629.
16. Roscoe TT, Guilleminot J, Bessoule J-J, Berger F, Devic M. Complementation of seed maturation phenotypes by ectopic expression of ABSCISIC ACID INSENSITIVE3, FUSCA3 and LEAFY COTYLEDON2 in Arabidopsis. Plant Cell Physiol. 2015;56(6):1215–28. https://doi.org/10.1093/pcp/pcv049.

17. Suzuki M, McCarty DRJC. Functional symmetry of the B3 network controlling seed development. Curr Opin Plant Biol. 2008;11(5):548–53. https://doi.org/10.1016/j.pbi.2008.06.015.
18. Mu J, Tan H, Zheng Q, Fu F, Liang Y, Zhang J, Yang X, Wang T, Chong K, Wang X-JJP. LEAFY COTYLEDON1 is a key regulator of fatty acid biosynthesis in Arabidopsis. Plant Physiol. 2008;148(2):1042–54. https://doi.org/10.1104/pp.108.126342.
19. Wang H, Guo J, Lambert KN, Lin YJP. Developmental control of Arabidopsis seed oil biosynthesis. Planta. 2007;226:773–83. https://doi.org/10.1007/s00425-007-0524-0.
20. Sagar M, Chervin C, Mila I, Hao Y, Roustan J-P, Benichou M, Gibon Y, Biais B, Maury P, Latché A, et al. SlARF4, an Auxin Response Factor Involved in the Control of Sugar Metabolism during Tomato Fruit Development. Plant Physiol. 2013;161(3):1362–74. https://doi.org/10.1104/pp.113.213843.
21. Yuan Y, Xu X, Gong Z, Tang Y, Wu M, Yan F, Zhang X, Zhang Q, Yang F, Hu X, et al. Auxin response factor 6A regulates photosynthesis, sugar accumulation, and fruit development in tomato. Hortic Res. 2019;6:6. https://doi.org/10.1038/s41438-019-0167-x.
22. Wang W, Li Y, Cai C, Zhu Q. Auxin response factors fine-tune lignin biosynthesis in response to mechanical bending in bamboo. New Phytol. 2024;241(3):1161–76. https://doi.org/10.1111/nph.19398.
23. Hu M, Zhang H, Wang B, Song Z, Gao Y, Yuan C, Huang C, Zhao L, Zhang Y, Wang L, et al. Transcriptomic analysis provides insights into the *AUXIN RESPONSE FACTOR* 6-mediated repression of nicotine biosynthesis in tobacco (*Nicotiana tabacum* L.). New Phytol. 2021;107(1):21–36. https://doi.org/10.1007/s11103-021-01175-3.
24. Iwakawa H-o, YJMc T. Molecular insights into microRNA-mediated translational repression in plants. Mol Cell. 2013;52(4):591–601. https://doi.org/10.1016/j.molcel.2013.10.033.
25. Dugas DV, Bartel BJC. MicroRNA regulation of gene expression in plants. Curr Opin Plant Biol. 2004;7(5):512–20. https://doi.org/10.1016/j.pbi.2004.07.011.
26. Meng Y, Ma X, Chen D, Wu P, Chen MJB. Communications br: MicroRNA-mediated signaling involved in plant root development. Biochem Biophys Res Commun. 2010;393(3):345–9. https://doi.org/10.1016/j.bbrc.2010.01.129.
27. Bologna NG, Mateos JL, Bresso EG, Palatnik JF. A loop-to-base processing mechanism underlies the biogenesis of plant microRNAs miR319 and miR159. EMBO J. 2009;28(23):3646–56. https://doi.org/10.1038/emboj.2009.292.
28. Palatnik JF, Allen E, Wu X, Schommer C, Schwab R, Carrington JC, Weigel DJN. Control of leaf morphogenesis by microRNAs. Nature. 2003;425(6955):257–63. https://doi.org/10.1038/nature01958.
29. Spanudakis E, Jackson SJJ. The role of microRNAs in the control of flowering time. J Exp Bot. 2014;65(2):365–80. https://doi.org/10.1093/jxb/ert453.
30. Martin RC, Liu P-P, Goloviznina NA. Nonogaki HJJoeb: microRNA, seeds, and Darwin? Diverse function of miRNA in seed biology and plant responses to stress. J Exp Bot. 2010;61(9):2229–34. https://doi.org/10.1093/jxb/erq063.
31. Bai B, Shi B, Hou N, Cao Y, Meng Y, Bian H, Zhu M, Han NJB. microRNAs participate in gene expression regulation and phytohormone cross-talk in barley embryo during seed development and germination. BMC Plant Biol. 2017;17:1–16. https://doi.org/10.1186/s12870-017-1095-2.
32. Dhaka N, Sharma RJCRB. MicroRNA-mediated regulation of agronomically important seed traits: a treasure trove with shades of grey! Crit Rev Biotechnol. 2021;41(4):594–608. https://doi.org/10.1080/07388551.2021.1873238.
33. Mallory AC, Dugas DV, Bartel DP, Bartel BJCB. MicroRNA regulation of NAC-domain targets is required for proper formation and separation of adjacent embryonic, vegetative, and floral organs. Curr Biol. 2004;14(12):1035–46. https://doi.org/10.1016/j.cub.2004.06.022.
34. Belide S, Petrie JR, Shrestha P, Singh SPJF. Modification of seed oil composition in Arabidopsis by artificial microRNA-mediated gene silencing. Front Plant Sci. 2012;3: 168. https://doi.org/10.3389/fpls.2012.00168.
35. Li J, Ding J, Yu X, Li H. Ruan CJIc, products: identification and expression analysis of critical microRNA-transcription factor regulatory modules related to seed development and oil accumulation in developing Hippophae rhamnoides seeds. Ind Crops Prod. 2019;137:33–42. https://doi.org/10.1016/j.indcrop.2019.05.011.
36. Gao LC, Wang YF, Zhu Z, Chen H, Sun RH, Zheng YS, Li DD. EgmiR5179 from the mesocarp of oil palm (*Elaeis guineensis* Jacq.) Regulates oil accumulation by targeting *NAD transporter 1*. Ind Crops Prod. 2019;137:126–36. https://doi.org/10.1016/j.indcrop.2019.05.013.
37. Dai X, Lu Q, Wang J, Wang L, Xiang F, Liu Z. MiR160 and its target genes *ARF10*, *ARF16* and *ARF17* modulate hypocotyl elongation in a light, BRZ, or PAC-dependent manner in Arabidopsis: miR160 promotes hypocotyl elongation. Plant Sci. 2021;303: 110686. https://doi.org/10.1016/j.plantsci.2020.110686.
38. Huang J, Li Z, Zhao D. Deregulation of the OsmiR160 target gene *OsARF18* causes Growth and Developmental defects with an alteration of Auxin Signaling in Rice. Sci Rep. 2016;6(1): 29938. https://doi.org/10.1038/srep29938.
39. Ding Y, Ma Y, Liu N, Xu J, Hu Q, Li Y, Wu Y, Xie S, Zhu L, Min L, et al. microRNAs involved in auxin signalling modulate male sterility under high-temperature stress in cotton (*Gossypium hirsutum*). Plant J. 2017;91(6):977–94. https://doi.org/10.1111/tpj.13620.
40. Zhang H, Chen H, Hou Z, Xu L, Jin W, Liang Z. Overexpression of AthMIR160b increased the biomass while reduced the content of tanshinones in *Salvia miltiorrhiza* hairy roots by targeting *ARFs* genes. Plant Cell Tissue Organ Cult (PCTOC). 2020;142(2):327–38. https://doi.org/10.1007/s11240-020-01865-8.
41. Shen EM, Singh SK, Ghosh JS, Patra B, Paul P, Yuan L, Pattanaik S. The miRNAome of *Catharanthus roseus*: identification, expression analysis, and potential roles of microRNAs in regulation of terpenoid indole alkaloid biosynthesis. Sci Rep. 2017;7(1): 43027. https://doi.org/10.1038/srep43027.
42. Wang Y, Liu W, Wang X, Yang R, Wu Z, Wang H, Wang L, Hu Z, Guo S, Zhang H, et al. MiR156 regulates anthocyanin biosynthesis through SPL targets and other microRNAs in Poplar. Hortic Res. 2020;7:7. https://doi.org/10.1038/s41438-020-00341-w.
43. Wang W-B, Ao T, Zhang Y-Y, Wu D, Xu W, Han B, Liu A-ZJPD. Genome-wide analysis of the B3 transcription factors reveals that RcABI3/VP1 subfamily plays important roles in seed development and oil storage in castor bean (*Ricinus communis*). Plant Divers. 2022;44(2):201–12. https://doi.org/10.1016/j.pld.2021.06.008.
44. Qu J, Wang B, Xu Z, Feng S, Tong Z, Chen T, Zhou L, Peng Z, Ding C. Genome-wide analysis of the molecular functions of B3 superfamily in oil biosynthesis in olive (Olea europaea L.). Biomed Res Int. 2023;2023(1):6051511. https://doi.org/10.1155/2023/6051511.
45. Wei M, Li H, Wang Q, Liu R, Yang L, Li QJFPS. Genome-wide identification and expression profiling of B3 transcription factor genes in *Populus alba*× *Populus glandulosa*. Front Plant Sci. 2023;14: 1193065. https://doi.org/10.3389/fpls.2023.1193065.
46. Ren C, Wang H, Zhou Z, Jia J, Zhang Q, Liang C, Li W, Zhang Y, Yu GJFPS. Genome-wide identification of the *B3* gene family in soybean and the response to melatonin under cold stress. Front Plant Sci. 2023;13: 1091907. https://doi.org/10.3389/fpls.2022.1091907.
47. Lu J-X, Sun J-Y, Wang Z, Ren W-C, Xing N-N, Liu M-Q, Zhang Z-P, Kong L-Y, Su X-Y, Liu X-BJC, et al. *Silico* Genome-Wide Analysis of B3 Transcription Factors in *Cannabis sativa* L. Cannabis Cannabinoid Res. 2024;9(2):495–512. https://doi.org/10.1089/can.2022.0168.
48. Ruan CC, Chen Z, Hu FC, Fan W, Wang XH, Guo LJ, Fan HY, Luo ZW, Zhang ZL. Genome-wide characterization and expression profiling of B3 superfamily during ethylene-induced flowering in pineapple (Ananas comosus L.). BMC Genomics. 2021;22:1–12. https://doi.org/10.1186/s12864-021-07854-1.
49. Santos-Mendoza M, Dubreucq B, Baud S, Parcy F, Caboche M, Lepiniec LJTPJ. Deciphering gene regulatory networks that control seed development and maturation in Arabidopsis. Plant J. 2008;54(4):608–20. https://doi.org/10.1111/j.1365-313X.2008.03461.x.
50. Liu P-P, Montgomery TA, Fahlgren N, Kasschau KD, Nonogaki H, Carrington JC. Repression of *AUXIN RESPONSE FACTOR10* by microRNA160 is critical for seed germination and post-germination stages. Plant J. 2007;52(1):133–46. https://doi.org/10.1111/j.1365-313X.2007.03218.x.
51. Huang D, Koh C, Feurtado JA, Tsang EWT, Cutler AJ. MicroRNAs and their putative targets in *Brassica napusseed* maturation. BMC Genomics. 2013;14(1):140. https://doi.org/10.1186/1471-2164-14-140.
52. Kandeel M, Morsy MA, Abd El-Lateef HM, Marzok M, El-Beltagi HS, Al Khodair KM, Albokhadaim I, Venugopala KN. Genome-wide identification of B3 DNA-Binding Superfamily Members (ABI, HIS, ARF, RVL, REM) and their involvement in stress responses and development in *Camelina sativa*. Agronomy. 2023;13(3):648. https://doi.org/10.3390/agronomy13030648.

53. Wang L, Chen F, Lan Y, Liu H, Wu M, Yan H, Xiang YJSH. Genome-wide identification of B3 superfamily in pecan (Carya Illinoensis): in silico and experimental analyses. Sci Hortic. 2023;307: 111533. https://doi.org/10.1016/j.scienta.2022.111533.
54. Romanel EA, Schrago CG, Couñago RM, Russo CA, Alves-Ferreira M. Evolution of the B3 DNA binding superfamily: new insights into REM family gene diversification. PLoS ONE. 2009;4(6):e5791. https://doi.org/10.1371/journal.pone.0005791.
55. Ahmad B, Zhang S, Yao J, Rahman MU, Hanif M, Zhu Y, Wang XJIJMS. Genomic organization of the B3-domain transcription factor family in grapevine (*Vitis vinifera* L.) and expression during seed development in seedless and seeded cultivars. Int J Mol Sci. 2019;20(18): 4553. https://doi.org/10.3390/ijms20184553.
56. Niu F, Ji C, Liang Z, Guo R, Chen Y, Zeng Y, Jiang LJPP. ADP-ribosylation factor D1 modulates golgi morphology, cell plate formation, and plant growth in Arabidopsis. Plant Physiol. 2022;190(2):1199–213. https://doi.org/10.1093/plphys/kiac329.
57. Ghelli R, Brunetti P, Marzi D, Cecchetti V, Costantini M, Lanzoni-Rossi M, Scaglia Linhares F, Costantino P, Cardarelli M. The full-length Auxin Response factor 8 isoform ARF8. 1 controls pollen cell wall formation and directly regulates *TDF1*, *AMS* and *MS188* expression. Plant J. 2023;113(4):851–65. https://doi.org/10.1111/tpj.16089.
58. Qin Y, Wang W, Chang M, Yang H, Yin F, Liu YJH. The PpIAA5-ARF8 Module regulates Fruit Ripening and Softening in Peach. Horticulturae. 2023;9(10): 1149. https://doi.org/10.3390/horticulturae9101149.
59. Yang Z, Liu X, Wang K, Li Z, Jia Q, Zhao C, Zhang M. ABA-INSENSITIVE 3 with or without FUSCA3 highly up-regulates lipid droplet proteins and activates oil accumulation. J Exp Bot. 2021;73(7):2077–92. https://doi.org/10.1093/jxb/erab524.
60. Che N, Yang Y, Li Y, Wang L, Huang P, Gao Y, An CJSCSCLS. Efficient LEC2 activation of *OLEOSIN* expression requires two neighboring RY elements on its promoter. Sci China Life Sci. 2009;52:854–63. https://doi.org/10.1007/s11427-009-0119-z.
61. Mallory AC, Bartel DP, Bartel BJTPC. MicroRNA-directed regulation of Arabidopsis *AUXIN RESPONSE FACTOR*$_{17}$ is essential for proper development and modulates expression of early auxin response genes. Plant Cell. 2005;17(5):1360–75. https://doi.org/10.1105/tpc.105.031716.
62. Liu N, Wu S, Li Z, Khan AQ, Hu H, Zhang X, Tu LJTCJ. Repression of microRNA 160 results in retarded seed integument growth and smaller final seed size in cotton. Crop J. 2020;8(4):602–12. https://doi.org/10.1016/j.cj.2019.12.004.
63. Wójcik AM, Nodine MD, Gaj MDJFPS. miR160 and miR166/165 contribute to the *LEC2*-mediated auxin response involved in the somatic embryogenesis induction in Arabidopsis. Front Plant Sci. 2017;8:283846. https://doi.org/10.3389/fpls.2017.02024.
64. Zhao Y, Luo Y, Chen Y, Ao Y. Products: integration of miRNA and *ARF* gene analysis provides a reference for the pistil abortion mechanism in *Xanthoceras sorbifolium*. Ind Crops Prod. 2024;212:118289. https://doi.org/10.1016/j.indcrop.2024.118289.
65. Qiao J, Jiang H, Lin Y, Shang L, Wang M, Li D, Fu X, Geisler M, Qi Y, Gao Z, et al. A novel miR167a-*OsARF6*-*OsAUX3* module regulates grain length and weight in rice. Mol Plant. 2021;14(10):1683–98. https://doi.org/10.1016/j.molp.2021.06.023.
66. Zhao Z-X, Yin X-X, Li S, Peng Y-T, Yan X-L, Chen C, Hassan B, Zhou S-X, Pu M, Zhao J-H, et al. miR167d-ARFs Module regulates Flower opening and stigma size in Rice. Rice. 2022;15(1):40. https://doi.org/10.1186/s12284-022-00587-z.
67. Shen X, He J, Ping Y, Guo J, Hou N, Cao F, Li X, Geng D, Wang S, Chen P, et al. The positive feedback regulatory loop of miR160-Auxin response factor 17-HYPONASTIC LEAVES 1 mediates drought tolerance in apple trees. Plant Physiol. 2021;188(3):1686–708. https://doi.org/10.1093/plphys/kiab565.
68. Alves A, Confraria A, Lopes S, Costa B, Perdiguero P, Milhinhos A, Baena-González E, Correia S, Miguel CM. miR160 interacts in vivo with Pinus pinaster AUXIN RESPONSE FACTOR 18 Target Site and negatively regulates its expression during Conifer somatic embryo development. Front Plant Sci. 2022;13. https://doi.org/10.3389/fpls.2022.857611.
69. Jiang W, Xia Y, Su X, Pang Y. ARF2 positively regulates flavonols and proanthocyanidins biosynthesis in *Arabidopsis thaliana*. Planta. 2022;256(2):44. https://doi.org/10.1007/s00425-022-03936-w.
70. Wang C, Li X, Zhuang Y, Sun W, Cao H, Xu R, Kong F, Zhang D. A novel miR160a–GmARF16–GmMYC2 module determines soybean salt tolerance and adaptation. New Phytol. 2024;241(5):2176–92. https://doi.org/10.1111/nph.19503.
71. Liu H, Chen S, Wu X, Li J, Xu C, Huang M, Wang H, Liu H, Zhao Z. Identification of the NAC transcription factor family during early seed development in *Akebia trifoliata (Thunb) Koidz*. Plants. 2023;12(7):1518. https://doi.org/10.3390/plants12071518.

Publisher's note